We have addressed peer-referees' comments and put together this authors' response document for *acp-2018-1015*, which includes detailed responses to all the referees and a revised change-tracked manuscript and supplementary material.

Response to Referee #1

Comments are in black and responses are in blue.

The authors provide an interesting and comprehensive analysis of the likely contributions of hydroxymethanesulfonate (HMS) to Beijing PM_1. This is a nice example of combining fascinating but often forgotten atmospheric chemistry of hydroxyalkylsulfonates from the 1980s and 90s with modern aerosol mass spectrometry techniques. Through the use of HR-AMS, single particle aerosol mass spec, and model simulations, the authors make a compelling case that HMS likely contributes significantly to the sulfur content of Beijing PM_1 during humid winter haze conditions. There are a few points that the authors should consider to improve the manuscript:

We thank Dr. Collett for commenting on this manuscript. Our responses to the specific comments and corresponding revisions made in the revised manuscript are provided below:

1. bottom of p. 9: The authors suggest that a good positive correlation between OS and AWC suggests that aerosol water is key to enabling OS production. One needs to be careful of using correlations to infer causation. My guess is that many Beijing PM_1 aerosol species are positively correlated with AWC, both because humid conditions tend to accompany haze events and because AWC depends explicitly on hygroscopic aerosol mass. Is the correlation of OS and AWC higher than for other species (e.g., NH_4NO_3)?

First, the correlation of OS and AWC ($r = 0.82$) was higher than that of nitrate (NO_3) and AWC ($r = 0.69$), as shown in the figure below (*left*: OS vs. AWC, *right*: NO_3 vs. AWC). Second, it is also noted from this figure that the intercepts of the linear regressions are different (a small value of 0.19 µg m^{-3} for OS vs. AWC whereas a larger value of 5.8 µg m^{-3} for NO_3). This may further imply the causal link between OS and AWC (when there is little AWC, there is little OS). NO_3 is known to be formed through different gaseous and heterogeneous pathways (e.g., $OH + NO_2$ and N_2O_5 hydrolysis). The correlation between NO_3 and AWC could primarily reflect the complex relationships among moisture and physical/chemical evolutions during haze events, as mentioned in the referee's comments.
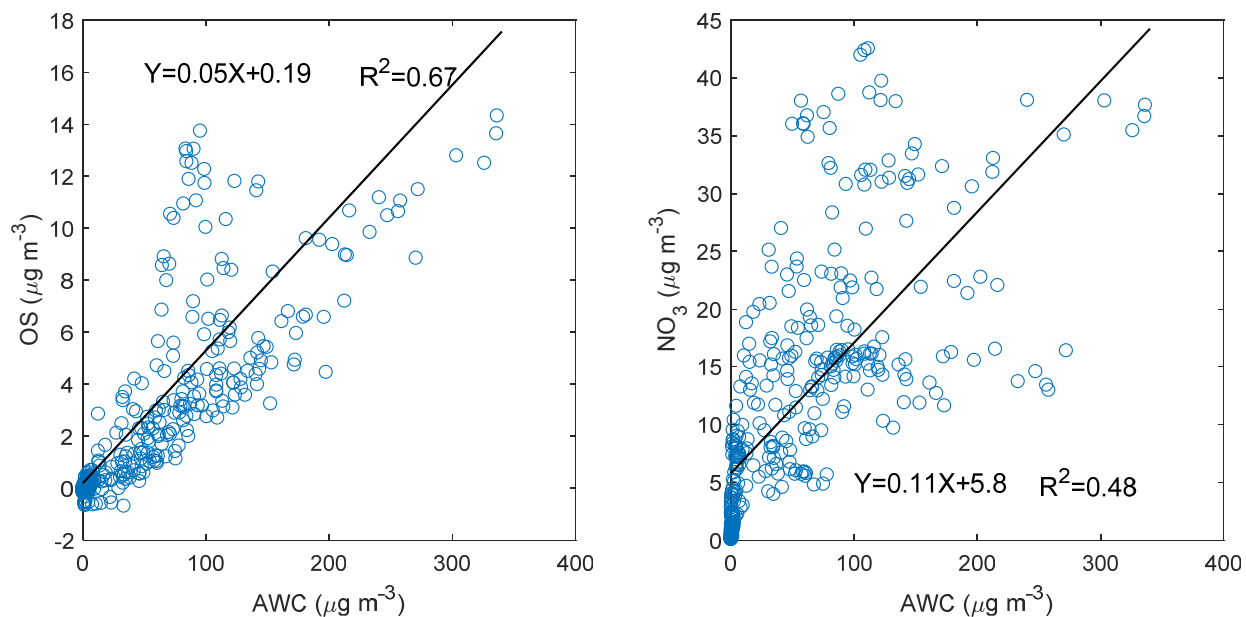
The small intercept of OS vs. AWC is partly because we used fragmentation patterns of inorganic sulfur ($H_xSO_y^+$) to derive OS levels. The figure below shows the variations of SO^+ fragment concentrations and SO^+/SO_3^+ fragmentation ratios. We can see that there is a good exponential relationship between SO^+ and RH, and that the ratios of SO^+/SO_3^+ did not change much under a RH of about 50% but increased quickly above that RH. This critical RH is deliquesced RH value under Beijing winter haze conditions, as predicted in our previous paper using thermodynamic equilibrium analyses (*Song et al. 2018 ACP, Fine-particle pH for Beijing winter haze as inferred from different thermodynamic equilibrium models, doi:10.5194/acp-18-7423-2018*). This may suggest that the existence of OS is associated with wet aerosols.
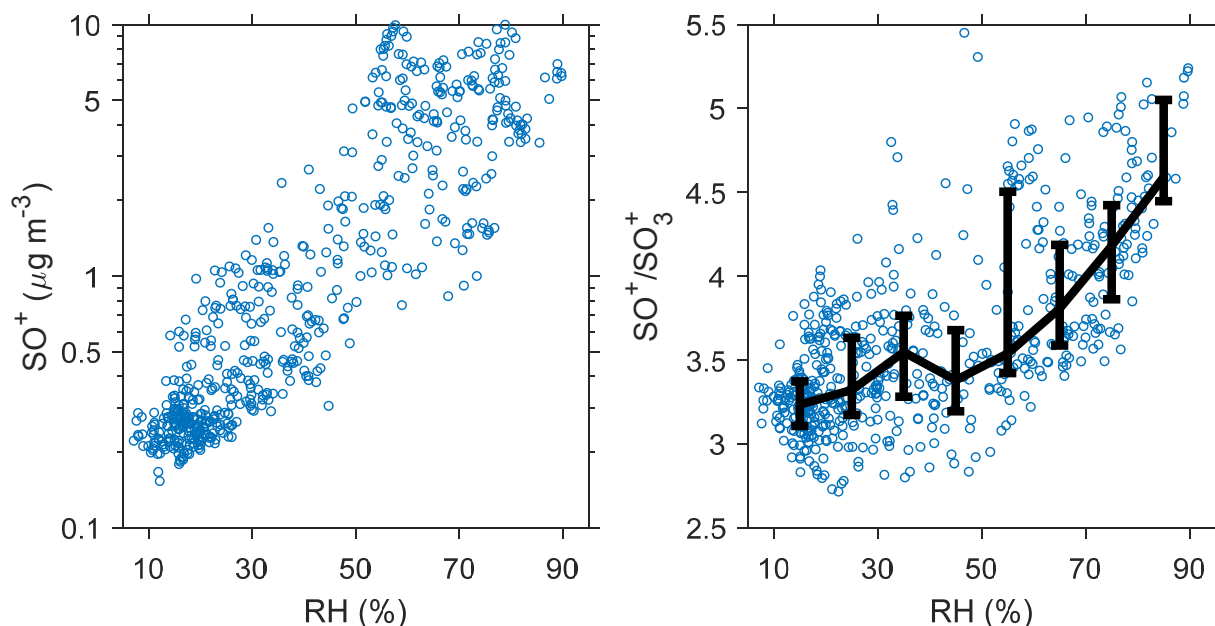
Note: the error bars in the right panel show 25% and 75% percentile, and the curve shows the median (50% percentile).

2. bottom of p. 11: The addition of the SPAMS data, although just for one event when available, greatly adds to the case that HMS is important in this environment. I am puzzled, however, by the observation that the HMS m/z 111

signature was observed in just 10% of particles. If AWC is the main ingredient needed, why isn't HMS contained in most of the particles? I suspect that most Beijing haze particles have substantial AWC in these events. Perhaps differences in pH across particles are important. The authors predict a single pH for PM1 assuming an internal mixture when the aerosol may really be externally mixed. Do the SPAMS data suggest that the HMS occurs in particles of a certain type (e.g., mineral dust particles) that might have a higher pH than other particle types? Are there HR-AMS P-TOF data that can inform us about the HMS size distribution?

The detection of HMS (with the characteristic ion peak at m/z -111) by the SPAMS (using 266 nm Nd:YAG laser for ionization) is subject to matrix effect: HMS ions may be fragmented into smaller ions such as HSO_3^- and SO_3^-, depending on the countercations in sampling particles (as described briefly in Sect. 3.4). Several previously published papers (e.g., Neubauer et al., 1997; Whiteaker and Prather, 2003) have discussed this phenomenon. For example, the salt of NaHMS does not produce the m/z -111 peaks at all (fragmented into SO_2^- and SO_3^-). The existence of $(NH_4)_2SO_4$ leads to the generation of m/z -111 ion peak, but relative signals (m/z -111:-97 peak area ratio vs. NaHMS: $(NH_4)_2SO_4$) are usually much smaller than unity. For another example, 10% NaHMS in aqueous particles in the mixture of NaHMS and $(NH_4)_2SO_4$ has m/z -111:-97 peak ratios of only 1-3%. The heterogeneity of pH and AWC values among different types of particles is another factor leading to the observed HMS frequency, as the referee has suggested.

We have AMS PToF data in this study as shown below. However, it is very challenging to derive the HMS size distributions from AMS PToF data because fragmentation of HMS and sulfate produces the same SO^+ and SO_2^+ ions. In the future, it could be possible to estimate the size distributions of HMS by comparing the size differences between SO^+/SO_2^+ and SO_3^+. As shown below, the average size distribution of sulfate presented a large and broad accumulation mode peaking at ~500 – 600 nm during the severe episode on 9 December (12:00 – 24:00). It is likely that HMS shared the similar size distribution to that of sulfate.
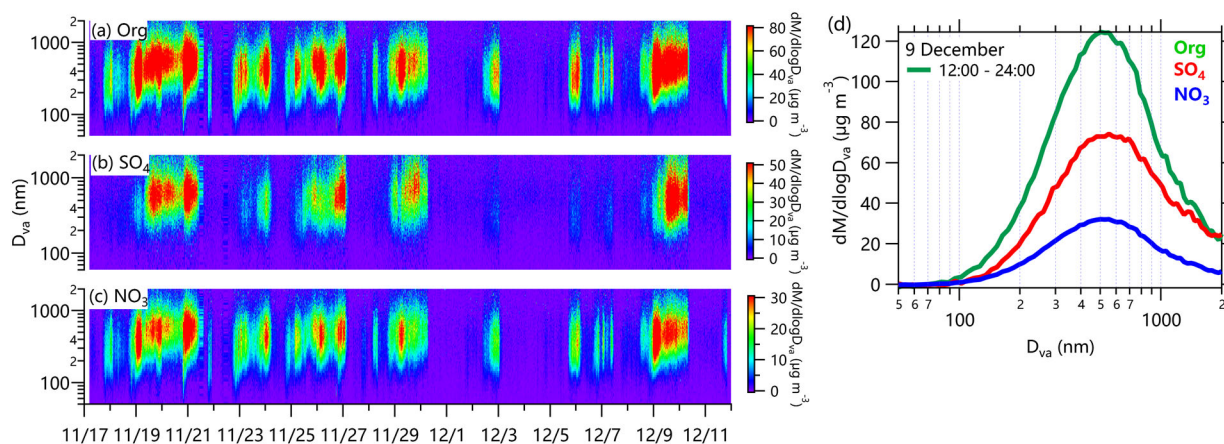

Figure. (a-c) Time series of size distributions of organics, sulfate, and nitrate for the entire study, and (d) average size distributions between 12:00 and 24:00 on 9 December.

3. If there are not aerosol pH-driven differences in HMS production that result in HMS being observed in just a small fraction of particles, perhaps cloud processing is important after all and the HMS was formed in subset of aerosol particles that underwent cloud processing elsewhere in the NCP before being transported to Beijing...?

As described in the earlier comment and response, the fraction of HMS-detected aerosol particles may not necessarily suggest heterogeneity in pH or AWC. But we agree with the referee that HMS may be formed in the subset of aerosol particles that undergo cloud processing before being transported to the observational station. Investigating this hypothesis requires simulations employing a three-dimensional chemical transport model. In the revised manuscript, we have added this hypothesis in the section (Sect. 3.5) discussing future research (see *Page 13 Lines 25-29*):

> "*In addition, three-dimensional chemical transport model studies should be conducted to further explore the HMS formation pathways and the associated uncertainties (e.g., pH values). The modeling simulations may*

also demonstrate whether significant amount of HMS can be formed in cloud droplets before transported to the ground level".

We should check whether the model results can reproduce the characteristics observed by mass spectrometry. Given the good relationship found between AWC and OS, we believe aerosol water provides space for the formation of HMS.

4. middle of p. 11: It would be helpful if the authors explained and justified their use of a modified HCHO emissions inventory here (or in the Methods section earlier), rather than leaving that explanation to the last page of the manuscript.

Based on the referee's suggestion, we have moved the explanation for the modified formaldehyde emissions to the Method section. The Results and Discussion section has also been changed accordingly. See revised manuscript *Page 7 Lines 15-23*:

> *"We conducted two model simulations: (1) a BASE scenario with normal settings; (2) a 5×EMIS scenario in which primary HCHO emissions from the transportation sector was elevated by a factor of 5. This is because, as described in Sect. 3 (Results and discussion), the BASE scenario significantly underestimated ambient HCHO concentrations. It remains unclear whether primary or secondary sources of HCHO are responsible for its high wintertime levels. Jobson and colleagues have recently suggested that HCHO emissions during motor vehicle cold starts, especially in cold winter, are significantly underestimated in current inventories (Jobson et al., 2017). Accordingly, a 5×EMIS scenario with increasing primary HCHO emissions from transportation was conducted, which greatly reduces the negative biases in the modeled HCHO and thus was used to calculate the formation rate of HMS."*

5. It would be interesting to look at the competition of aqueous sulfate and HMS formation in Beijing AWC. Both formaldehyde and various oxidants are competing for dissolved S(IV) in the wet aerosol particles. How do the relative rates of HMS and sulfate production change with aerosol pH and plausible concentrations of reactants and catalysts? The aerosol droplets are small enough and the SO_2 likely abundant enough, that the S(IV) oxidation and HMS formation pathways can proceed in parallel, but their relative rates for typical Beijing winter haze conditions would be interesting to outline.

We agree with the referee that other chemical pathways consuming SO_2 may occur simultaneously in the wet aerosol particles. As described in the Introduction section of our manuscript, potential reactants may include dissolved NO_2, transition-metal-catalyzed O_2, H_2O_2, et al. This manuscript focused on the reaction of HCHO and SO_2, and we calculated the time scales of relevant physical and chemical processes. The below figure (Figure S10 in the Supplement) shows that the nucleophilic addition reaction (τ_r) is not limited by mass transfer ($\tau_{dg\&phase}$: gas diffusion and phase equilibrium), by aqueous diffusion (τ_{da}: aqueous diffusion), and by acid hydrolysis (τ_{i1} and τ_{i2}: two-step dissociation). The fast exchange of SO_2 from gas phase to aerosol-water-aqueous phase is primarily a result of small aerosol size, as also suggested by the referee, which also implies that the rates of different heterogeneous pathways are unlikely limited by the supply of SO_2.
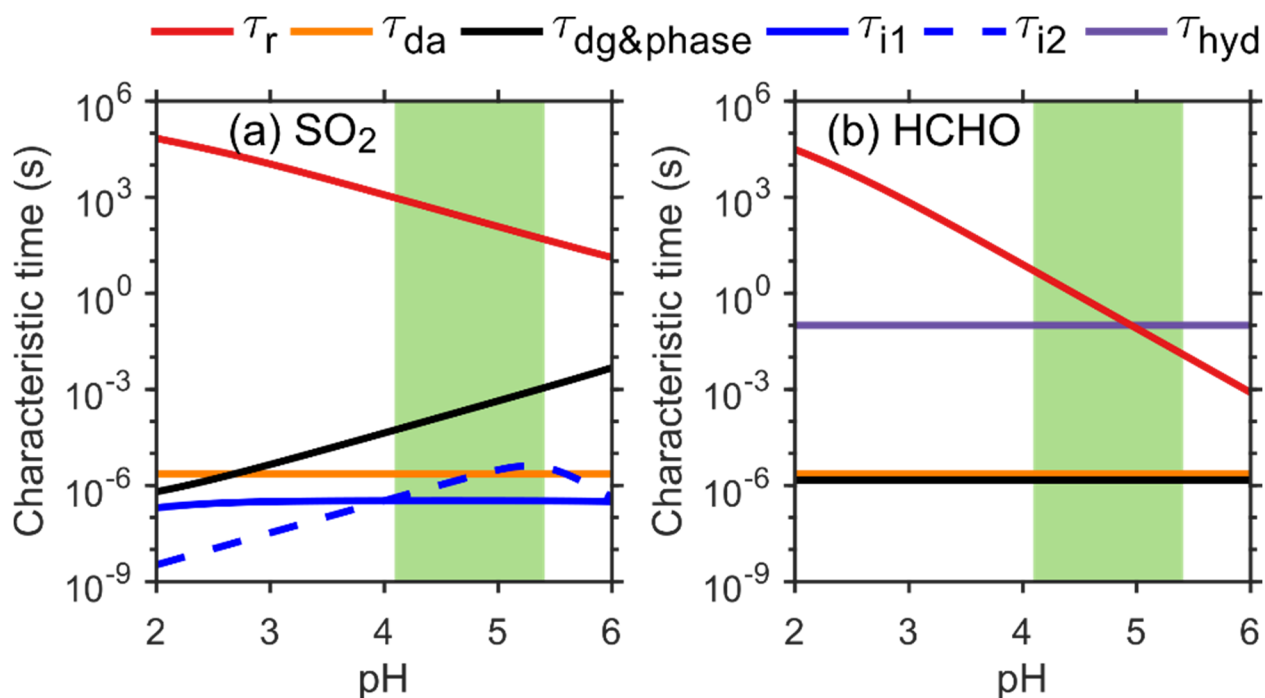
Quantitative analyses of the relative rates of different SO_2 reaction pathways are probably beyond the scope of this particular study. Several previously published papers have addressed several possible pathways and most of them have been referenced in the manuscript (see the Introduction section). A brief summary of these studies was also presented in Introduction:

> *"Their relative importance for sulfate production in winter haze, however, is unknown due to uncertainties in relevant reaction rates and estimates for aerosol water pH values (most reaction pathways are pH-dependent)"*.

The findings of this manuscript that HMS contributes up to one thirds of the missing sulfate imply that there are other potential pathways contributing to particulate sulfate. As suggested by the characteristic times in the above figure, mass transfer and acid dissociation of SO_2 are unlikely to be the limiting factor under the winter haze conditions.

6. The authors do not mention the recent Moch et al. GRL publication, involving several of the same authors that contribute to this paper, that takes a different look at HMS contributions to Beijing PM1. This is likely just a timing issue with submission of the two manuscripts, but should be corrected in production of a revised manuscript.

In the original manuscript, we cited Moch et al. 2017 poster in AGU 2017 (our paper came out earlier than their GRL paper and ACP journal did not allow cite paper under review). We have changed the citation to Moch et al. 2018 GRL in the revised manuscript. We did not find a relationship between the identified OS and local cloud/fog presence, as described in Sect. 3.1 and Fig. S5.

7. It would be useful for the authors to comment somewhere in the manuscript on the fate of HMS formed in wet haze particles if the RH drops enough for the particles to dry out. Will the HMS still be retained in the dry aerosol?

We have added a brief comment in Sect. 2.6 (*Kinetics and thermodynamics of HMS heterogeneous production*) on the fate of HMS when aerosols dry out. See *Page 9 Lines 10-12*:

> *"It is noted that $CH_2(OH)SO_3^-$ may form salts by the neutralization reaction with ammonium or other cations (e.g., Na^+, K^+, and Ca^{2+}) and undergo precipitation when the ambient RH becomes lower than the efflorescence RH value."*

Response to Eck

Comments are in black and responses are in blue.

There is additional indirect evidence of HMS production in China, from retrieved aerosol size distributions inferred from measurements made by sun-sky radiometers in the AERONET and associated networks. In these cases the HMS sized particles were observed only when fog or low altitude layer cloud events were associated with aerosol pollution. Specifically, two papers have been published regarding this topic, Eck et al. 2012 JGR (see especially Figs 4 and 14) and Li et al. 2014 in Atmospheric Environment.

We thank Mr. Tom Eck very much for commenting on this manuscript. We have added these two references into the revised manuscript:

Eck, T. F., et al. (2012), Fog- and cloud-induced aerosol modification observed by the Aerosol Robotic Network (AERONET), J. Geophys. Res., 117, D07206, doi: 10.1029/2011JD016839.

Li, Z., Eck, T., Zhang, Y., Zhang, Y., Li, D., Li, L., et al. (2014). Observations of residual submicron fine aerosol particles related to cloud and fog processing during a major pollution event in Beijing. Atmospheric Environment, 86, 187–192. https://doi.org/10.1016/j. atmosenv.2013.12.044

Eck et al. (2012) and Li et al. (2014) showed indirect evidence for the existence of HMS from the ground-based remote sensing measurements from the AERONET network. These measurements found in several cases that a fine mode with radius of 0.5 μm might be contributed by HMS, because the associated change was consistent with the observed features In the London fog event (Dall'Osto et al. 2009; cited in our manuscript). Dall'Osto et al. (2009) used the same measurement technique with our study, single particle mass spectrometry, to detect the contribution of HMS to *in situ* aerosol particles. In our cases in Beijing, results of the SPAMS measurements were qualitatively consistent with those from HR-AMS measurements (Fig. 3b). A relationship between HMS signals and local fog events were not observed (Fig. S6 in the revised supplementary).

Response to Referee #2

Comments are in black and responses are in blue.

This manuscript presents very interesting results for the organic sulfate production during haze periods in northern China. Results from this manuscript clearly showed that nearly all the sulfate measured can be attributed to inorganic sulfate during dry and clean periods while up to one third of total sulfate is attributed to organic sulfate (OS). Among them, hydroxymethanesulfonate (HMS) is likely the major OS species. The results are very intriguing and worthy of being further explored. However, several major issues need to be resolved before the manuscript can be publishable.

We thank the referee for commenting on this manuscript. Our responses to the specific comments and corresponding revisions made in the revised manuscript are provided below.

1. It seems the title is misleading. The major idea of this paper is to conclude that HMS is likely the major OS species as the results and discussion section clearly followed this logic. In addition, no clear conclusion can be made for rapid sulfate production or even oxidation of HMS which leads to the sulfate formation is still speculative. The chemistry itself is not new and all the reactions in the text were cited from literature. Based on this reason, I would suggest the authors to change the title of this paper to something like "Major contribution of Hydroxymethanesulfonate (HMS) to organic sulfate in northern China winter haze".

We agree with the referee that no clear conclusion is made for the oxidation of HMS to inorganic sulfate. The paper conveys two ideas: one is that HMS is likely a major and significant OS species (from a measurement perspective) and the other is that heterogeneous production of HMS by SO_2 and formaldehyde is favored under Beijing winter haze conditions (high aerosol water content, moderately acidic pH, high gaseous precursor levels, and low temperature) (from a modeling perspective). Combining the current knowledge on these two perspectives, we propose the potential importance of heterogeneous hydroxymethanesulfonate (HMS) chemistry in northern China winter haze. Accordingly, the title of the paper has been changed in the revised manuscript to:

"Possible heterogeneous chemistry of hydroxymethanesulfonate (HMS) in northern China winter haze"

2. The authors mentioned that HMS may serve as a reservoir for sulfate, if oxidation of HMS is rapid in the presence of aqueous OH radical, HMS will be quickly converted to sulfate which means that the formation of this intermediate is not important in term of the interpretation of sulfate from the AMS measurements, that is, sulfate from either this pathway or SO_2 oxidation is measured as inorganic sulfate. Only when HMS is present in a significant concentration, it becomes important as a major contributor to OS. The authors need to clarify this point.

We agree with the referee and have modified relevant sentences in Section 3.4 in order to clarify this point, see *Page 13 Lines 1-17*:

"HMS should exist as the $CH_2(OH)SO_3^-$ anion in wet aerosols and may form salts with ammonium or other cations when aerosol particles dry out. A possible fate of HMS is to be oxidized by aqueous OH radicals producing peroxysulfate radicals ($SO_5^{\bullet -}$) ...
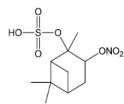
$SO_5^{\bullet -}$ is an intermediate in the free-radical chain reactions oxidizing SO_2 to SO_4^{2-}, and for each attack of OH on HMS, multiple SO_4^{2-} ions are produced (Fig. S8). Importantly, a HCHO molecule is released by reaction (17), suggesting that this reaction pathway does not result in net consumption of HCHO and that HMS serves as a temporary reservoir of tetravalent sulfur. We speculate from the diurnal patterns of HMS production rates (P_{HMS}) and the identified OS concentrations that oxidation of HMS by OH is likely to occur during daytime (Tan et al., 2018) (Fig. S8). But the rate of reaction (17) should be relatively slow when compared with that of reactions (10–11) because a significant level of HMS is expected to reside in the haze aerosol particles. A quantitative rate estimation for this pathway, however, is difficult, because aqueous OH is short-lived and it can be derived as a result of uptake from the gas phase or be generated or scavenged in the condensed phase (Jacob, 1986; Ervens et al., 2014)."

We note in the above paragraph that the oxidation of HMS by aqueous OH is currently merely a hypothesis/speculation given the previously reported mechanism and the relatively high level of gaseous OH during Beijing winter haze events. Only when HMS is present in a significant concentration, it becomes important as a major contributor to OS. The reaction of HMS and OH cannot be very fast to consume most formed HMS. It may also be important that each attach of HMS by OH has the potential to produce multiple inorganic sulfate.

3. In addition to HMS, the authors list several categories of organic sulfate including methanesulfonate, sulfones, and organosulfates etc. Are there still any other types of OS which might not be considered because of the limitation of the current measurement techniques? In addition, the authors mentioned that several common organosulfates were not detected by the SPAMS; however, that does not mean that they are not significantly present. It is possible that the SPAMS was not capable of detecting them due to its limitation measurement scheme.

This manuscript wrote in the Introduction section that: "*organosulfur compounds ... including organosulfates ($ROSO_3^-$), sulfones (RSO_2R'), and sulfonates (RSO_3^-) such as methanesulfonate ($CH_3SO_3^-$, the deprotonated anion of methanesulfonic acid, MSA) and hydroxyalkylsulfonates ($RCH(OH)SO_3^-$) (Eatough and Hansen, 1984; Dixon and Aasen, 1999; Surratt et al., 2008; Tolocka and Turpin, 2012; Sorooshian et al., 2015)*". To the best of our knowledge, these above chemical forms include all of the organic sulfur species that have been identified in ambient aerosols. The relative importance of different species varies among different seasons and locations. It should be noted that nitrooxy organosulfates were considered to fall in the scope of organosulfates due to the common sulfate functional group (e.g.,
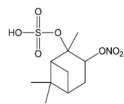
$C_{10}H_{17}NO_7S$ (proposed structure:), a type of secondary organic aerosol that may be formed by α/β-pinene; *Nguyen, Q. T., et al.: Understanding the anthropogenic influence on formation of biogenic secondary organic aerosols in Denmark via analysis of organosulfates and related oxidation products, Atmos. Chem. Phys., 14, 8961-8981, doi:10.5194/acp-14-8961-2014, 2014*).

The single particle mass spectrometry is a common measurement technique to detect the existence of organosulfate compounds, though it is not a suitable way to provide quantitative information for their mass concentrations. Field measurements using such technique have been conducted in many places around the world, for example by Hatch et al. 2011b (cited in our manuscript) in United States and by Wang et al. 2017 (added and cited in the revised manuscript) in China. We have clarified this point in the revised manuscript, see *Page 4 Lines 24-25*:

> *"The negative ion peaks at m/z -155, -187, -199, and -215 were also analyzed in order to detect individual organosulfate species. This technique has been employed to measure individual organosulfates in different regions around the world (Hatch et al., 2011a; Wang et al., 2017)."*

4. According to the thermodynamic rules, ammonia will be titrated before it can be taken up by nitrate aerosols. So why it bothers that these fragment ratios should be related to the ammonium nitrate? (line 25 on p5)

The potential influence of ammonium nitrate fraction on the fragmentation patterns of inorganic sulfur is mainly due to the mechanism of AMS measurements. In the preparation of the submitted manuscript, we have asked for and received many useful comments from several experts in the AMS measurements. One of them was that variations of inorganic sulfur fragmentation ratios might be related with the fraction of ammonium nitrate in aerosol particles. There exists a paper currently under peer review covering this issue (we cited this paper in our manuscript):

Chen, Y., Xu, L., Humphry, T., Hettiyadura, A., Ovadnevaite, J., Huang, S., Poulain, L., Campuzano-Jost, P., Schroder, J., Jimenez, J., Herrmann, H., O'Dowd, C., Stone, E., and Ng, N. L.: Response of the Aerodyne Aerosol Mass Spectrometer to inorganic sulfates and organosulfur compounds: applications in field and laboratory measurements, Environ. Sci. Technol., 2018, Submitted.

It has been known that the fraction of ammonium nitrate may affect the collection efficiency of AMS from laboratory and field experiments. This effect is related to the phase state of ammonium nitrate, which is a metastable liquid in the atmosphere at any sampling line RH. Middlebrook et al. (2012) (cited in our manuscript) provided a good summary of those experiments. The collection efficiency of AMS generally increases with enhanced fraction of ammonium nitrate. But this known effect should not change the fragmentation patterns of inorganic sulfur.

Middlebrook, A. M., Bahreini, R., Jimenez, J. L., and Canagaratna, M. R.: Evaluation of composition-dependent collection efficiencies for the Aerodyne aerosol mass spectrometer using field data, Aerosol Sci. Technol., 46, 258-271, doi:10.1080/02786826.2011.620041, 2012.

Because of the potential influence of ammonium nitrate, we choose to examine the observed relationship between the inorganic sulfur fragmentation patterns and ammonium nitrate fraction. Below is a figure showing this relationship. In the revised manuscript we have added it in the supplementary as *Figure S4*. This figure shows that there was not a clear relationship between ammonium nitrate fraction and the fragmentation ratios of inorganic sulfur from our field measurements. In addition, the fraction of ammonium nitrate was usually lower than 0.3.
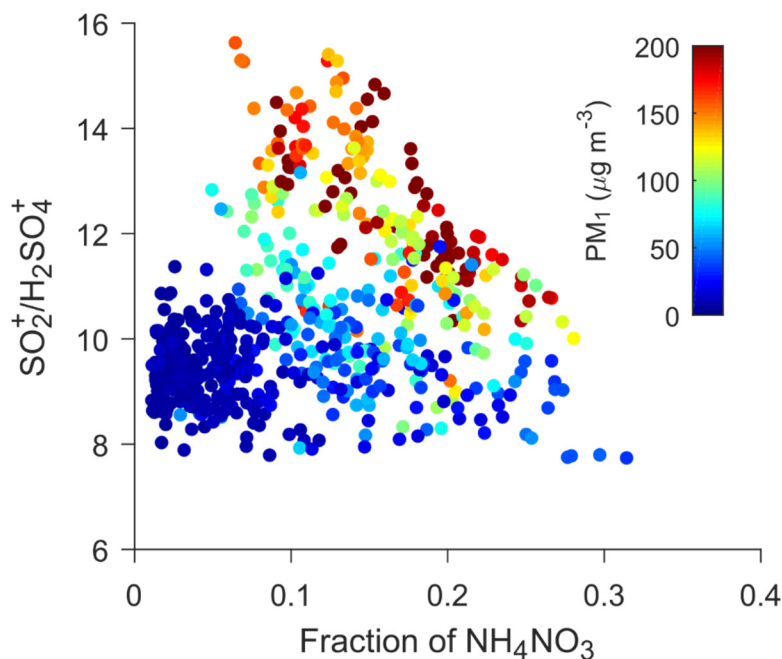
Figure. Relationship between $SO_2^+/H_2SO_4^+$ and fraction of ammonium nitrate. The dots are colored according to PM_1 mass concentrations.

Some minor comments

1. Fig. 2b doesn't show any information on the RH. Do you mean Fig. 2a-b?

Yes. Fig.2a-b respectively show the time series of measured RH and inorganic sulfur fragmentation ratio $SO^+/H_2SO_4^+$. We have changed the corresponding text in Sect. 2.2.

2. Line 4 on p6 here miss "to be" between "considered" and "the concentration"

We have added "to be" in the corresponding sentence in Sect. 2.2. This sentence in the revised manuscript is:

$$\text{``}\overline{R_{cd,SO^+/H_ySO_x^+}} \cdot H_ySO_{x,obs}^+ \text{ is considered to be the concentration of } SO^+ \text{ attributable to inorganic sulfate''}$$

3. Line 30 on p9 I don't think you can make cloud related statements since the periods are all covered by cloud

Haze periods are typically covered with clear sky. The blue color in the original figure of the supplementary represents clear sky. The original color scheme may be misleading, and thus we have modified the scheme in the supplementary figure, and have also added a legend for different colors, as shown below. Corresponding changes have been made in the revised manuscript.
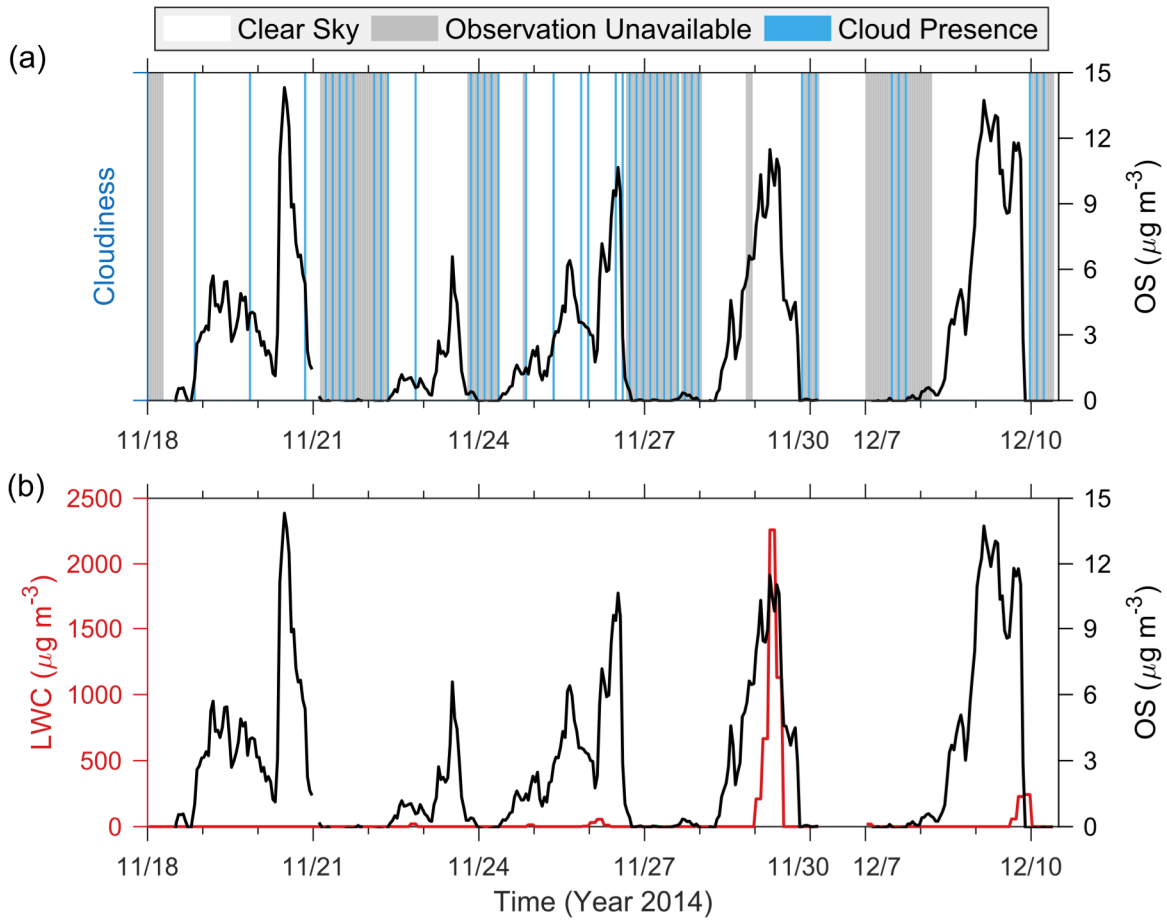
Figure. Relationship between the sulfate-equivalent OS concentrations and cloud/fog information in Beijing winter. (a) Time series of OS and cloud cover as observed at the Beijing Capital International Airport. Blue, white, and gray colors indicate cloud presence, clear sky, and observation unavailable, respectively. ... (b) Time series of OS and cloud/fog liquid water content (LWC) during 2014 winter in Beijing. ...

Possible heterogeneous ~~chemistry of~~ hydroxymethanesulfonate (HMS) ~~chemistry~~ in northern China winter haze ~~and implications for rapid sulfate formation~~

Shaojie Song[1*], Meng Gao[1], Weiqi Xu[2,3], Yele Sun[2,3,4*], Douglas R. Worsnop[5], John T. Jayne[5], Yuzhong Zhang[1], Lei Zhu[1], Mei Li[6,7], Zhen Zhou[6,7], Chunlei Cheng[6,7], Yibing Lv[8], Ying Wang[9], Wei Peng[9], Xiaobin Xu[9], Nan Lin[10], Yuxuan Wang[11], Shuxiao Wang[12], J. William Munger[1], Daniel J. Jacob[1], Michael B. McElroy[1*]

[1]School of Engineering and Applied Sciences, Harvard University, Cambridge, MA 02138, USA
[2]State Key Laboratory of Atmospheric Boundary Physics and Atmospheric Chemistry, Institute of Atmospheric Physics, Chinese Academy of Sciences, Beijing 100029, China
[3]College of Earth Sciences, University of Chinese Academy of Sciences, Beijing 100049, China
[4]Center for Excellence in Regional Atmospheric Environment, Institute of Urban Environment, Chinese Academy of Sciences, Xiamen 361021, China
[5]Aerodyne Research, Inc., Billerica, MA 01821, USA
[6]Institute of Mass Spectrometer and Atmospheric Environment, Jinan University, Guangzhou 510632, China
[7]Guangdong Provincial Engineering Research Center for Online Source Apportionment System of Air Pollution, Guangzhou 510632, China
[8]China National Environmental Monitoring Center, Beijing 100012, China
[9]State Key Laboratory of Severe Weather & Key Laboratory for Atmospheric Chemistry of CMA, Chinese Academy of Meteorological Sciences, Beijing 100081, China
[10]Department of Earth System Science, Tsinghua University, Beijing 100084, China
[11]Department of Earth and Atmospheric Sciences, University of Houston, Houston, TX 77004, USA
[12]School of Environment, Tsinghua University, Beijing 100084, China

Correspondence to: Shaojie Song (songs@seas.harvard.edu), Yele Sun (sunyele@mail.iap.ac.cn), Michael B. McElroy (mbm@seas.harvard.edu)

Abstract. Chemical mechanisms responsible for rapid sulfate production, an important driver of winter haze formation in northern China, remain unclear. Here, we propose a potentially important heterogeneous hydroxymethanesulfonate (HMS) chemical mechanism. Through analyzing field measurements with aerosol mass spectrometry, we show evidence for a possible significant existence in haze aerosols of organosulfur primarily as HMS, misidentified as sulfate in previous observations. We estimate that HMS can account for up to about one-third of the sulfate concentrations unexplained by current air quality models. ~~In addition, HMS in the presence of hydroxyl radicals can trigger rapid sulfate production in aerosol water.~~ Heterogeneous production of HMS by SO_2 and formaldehyde is favored under northern China winter haze conditions due to high aerosol water content, moderately acidic pH values, high gaseous precursor levels, and low temperature. These analyses identify an unappreciated importance of formaldehyde in secondary aerosol formation and calls for more research on sources and on the chemistry of formaldehyde in northern China winter.

1 Introduction

Severe haze episodes occur frequently in Beijing and throughout the North China Plain (NCP), especially in winter, posing substantial threats to public health (Ding et al., 2016; Fu and Chen, 2017; Gao et al., 2017). High concentrations of fine particles and reduced visibility are associated with stagnant meteorological conditions, i.e., shallow boundary layers, weak winds, and

5 high relative humidity (RH) (Wang et al., 2014a; Cai et al., 2017; Tie et al., 2017). Rapid formation of particulate sulfate is considered one of the key drivers of haze pollution for several reasons: sulfate is an important component of fine particles; it facilitates the partitioning of gaseous ammonia into the particle phase; and it enhances aerosol water uptake, changing the optical and chemical properties of aerosols (Guo et al., 2014; Huang et al., 2014). Sulfate is also known to impact climate and acid deposition (Charlson et al., 1992; Xie et al., 2015).

10

Most of the sulfate is of secondary origin, formed by oxidation of anthropogenic SO_2 (He et al., 2018). The exponential relationship between RH and the molar ratios of sulfate relative to SO_2, as observed during 2014 winter in Beijing (Fig. 1; see Methods) and in many previous studies (Sun et al., 2013; Zheng et al., 2015b; Wang et al., 2016), implies that heterogeneous chemistry (processes involving both gas and aerosol phases) plays an important role in production of sulfate. Indeed, air quality

15 model simulations fail to capture the rapid increase of sulfate from clean to haze periods when considering only the oxidation of SO_2 in the gas phase and in cloud/fog water, suggesting missing heterogeneous sources of sulfate (Wang et al., 2014b; Zheng et al., 2015a; Li et al., 2017a) (Fig. 1). Adding an apparent RH-dependent heterogeneous uptake for SO_2 on aerosols greatly reduces the negative bias in the modeled sulfate concentrations (see Methods) (Wang et al., 2014b; Zheng et al., 2015a).

20 Several heterogeneous reaction pathways have been proposed (He et al., 2014; Cheng et al., 2016; Wang et al., 2016; Li et al., 2017a; Hung et al., 2018; Qin et al., 2018; Yu et al., 2018), including oxidation of SO_2 in aerosol water (by NO_2, transition-metal-catalyzed O_2, or H_2O_2) and on aerosol surfaces (by NO_2 and/or O_2). Their relative importance for sulfate production in winter haze, however, is unknown due to uncertainties in relevant reaction rates and estimates for aerosol water pH values (most reaction pathways are pH-dependent) (Guo et al., 2017b; Liu et al., 2017a; Li et al., 2018b; Wang et al., 2018; Zhao et

25 al., 2018). For example, Wang et al. (2016; 2018) found in laboratory experiments that the rate for oxidation of SO_2 by NO_2 strongly depended on types of seed particles. In another example, Cheng et al. (2016) suggested that reactions of SO_2 with NO_2 in aerosol water could be the source of missing sulfate given the neutralized feature of haze aerosols (with a pH value of about 6 estimated with the ISORROPIA-II thermodynamic equilibrium model). Guo et al. (2017b) argued that the ISORROPIA-II calculation in Cheng et al. (2016) overestimated aerosol water pH, and that transition-metal-catalyzed O_2

30 instead of NO_2 was the key oxidant of SO_2.

Therefore, solution to the missing sulfate problem (discrepancy between observations and model results) in northern China winter haze remains challenging and controversial. The term sulfate in the atmospheric chemistry literature commonly refers

2

to inorganic sulfate species. In addition to inorganic sulfate, organosulfur compounds (OS) have also been demonstrated to be present in atmospheric aerosols, including organosulfates ($ROSO_3^-$), sulfones (RSO_2R'), and sulfonates (RSO_3^-) such as methanesulfonate ($CH_3SO_3^-$, the deprotonated anion of methanesulfonic acid, MSA) and hydroxyalkylsulfonates ($RCH(OH)SO_3^-$) (Eatough and Hansen, 1984; Dixon and Aasen, 1999; Surratt et al., 2008; Tolocka and Turpin, 2012; Sorooshian et al., 2015). OS may have been misidentified as inorganic sulfate in previous ambient measurements, thus leading to a positive observational bias (as described later). The formation of OS is typically not included in air quality model simulations, and thus can partly explain the missing sulfate problem if concentrations of these species are appreciable. However, OS concentrations in northern China winter haze aerosols have rarely been reported, and their formation mechanisms are also unknown.

In this study, we interpreted measurement data collected by a high-resolution time-of-flight aerosol mass spectrometer (HR-AMS) and a single particle aerosol mass spectrometer (SPAMS) in Beijing winter. We demonstrated the possible presence of OS in haze aerosols and discussed the potential of different OS species. Hydroxymethanesulfonate (HMS, $CH_2(OH)SO_3^-$) was found likely to be the primary OS component. We found that heterogeneous production rate of HMS through reaction of formaldehyde (HCHO) and SO_2 was fast enough to account for the identified OS by HR-AMS. Furthermore, we hypothesized that HMS might lead to additional sulfate production through a mechanism involving aqueous hydroxyl radicals (OH). Finally, we discussed the implications of this heterogeneous HMS chemical mechanism for the missing sulfate problem and also future research needs.

2 Methods

2.1 Field measurements

Aerosol and gaseous pollutants were measured in urban Beijing during winter 2014 (mid-November to mid-December) (Fig. S1). Chemical composition of non-refractory PM_1 was measured by a HR-AMS (Aerodyne Research, Inc., USA). Individual particles (0.2–2 μm) were detected by a SPAMS (Hexin Analytical Instrument Co., China). The Gas and Aerosol Collector Ion Chromatography (GAC-IC) system determined the concentrations of semi-volatile gases (HNO_3, NH_3, and HCl), and commercial analyzers were used to measure black carbon (AE33, Magee Scientific, USA), gaseous HCHO (AL4021, Aero-Laser GmbH, Germany), and SO_2 and O_3 (Thermo Fisher Scientific Inc., USA). Meteorological data were also recorded. Details are provided below and in Table S1.

2.1.1 HR-AMS measurements

Particles were vaporized by impaction on a heated surface (600 °C) and the resulting vapors were ionized by an electron impact ionization source (70 eV) (DeCarlo et al., 2006; Sun et al., 2016). The positive fragment ions generated were detected then using time-of-flight mass spectrometry. The HR-AMS switched every five minutes between the mass sensitive V-mode (mass

3

resolution of ~2000) and the high resolution W-mode (mass resolution of ~4500). A default collection efficiency of 0.5 was assumed (Middlebrook et al., 2012), because the mass fraction of ammonium nitrate was below 40%, the aerosol particles were moderately acidic (Song et al., 2018), and a silica gel dryer was used to reduce RH in the sampling line. The ionization efficiency calibrations were performed using pure ammonium nitrate particles following Jayne et al. (2000), and the default

5 relative ionization efficiencies (RIE), except for ammonium that was calibrated by ammonium nitrate, were applied to all the chemical species for mass quantifications. It is noted that the calibrated RIE values of sulfate later in 2017 and 2018 ranged from 1.22 to 1.39 (unpublished data), implying a possible overestimation of sulfate mass concentrations by 2%–14%. Mass concentrations of chemical components (ammonium, sulfate, nitrate, chloride, and organics) and inorganic and organic sulfur-containing fragment ions ($H_ySO_x^+$ and $C_xH_yO_zS^+$) were quantified with the standard data analysis software packages (Sueper

10 and collaborators, 2018). These sulfur-containing ions were well separated from adjacent peaks in the observed mass spectra and thus quantified with high confidence (examples in Fig. S2). The uncertainty quantification of chemical species followed Bahreini et al. (2009) (details in Text S1).

2.1.2 SPAMS measurements

The SPAMS (Li et al., 2011) was based on the same principle as the ATOFMS (aerosol time-of-flight mass spectrometer)
15 designed by Prather et al. (1994). Ambient aerosol particles were introduced and focused into a narrow beam using an aerodynamic lens. Particles passed through two continuous 532 nm Nd:YAG lasers with velocities determined on the basis of observed travelling times. The individual particles were ionized using a 266 nm Nd:YAG laser, and both positive and negative ions were generated and detected by bipolar time-of-flight mass spectrometry. The Computational Continuation Core software framework based on MATLAB (The MathWorks, Inc., USA) was used to analyze these ions. The negative ion peak at *m/z*
20 −111 has been assigned to HMS ($CH_2(OH)SO_3^-$) with no significant interference from other species in previous laboratory and field studies (Lee et al., 2003; Whiteaker and Prather, 2003; Dall'Osto et al., 2009; Zhang et al., 2012). HMS-containing particles were identified by the presence of a peak at *m/z* −111 with the absolute and relative peak areas greater than 50 and 0.5%, respectively. The negative ion peaks at *m/z* −155, −187, −199, and −215 were also analyzed in order to detect individual organosulfate species. This technique has been employed to measure individual organosulfates in different regions around the
25 world (Hatch et al., 2011a; Wang et al., 2017).

2.1.3 HCHO measurements

The AL4021 analyzer is based on the Hantzsch reaction (HCHO reacts with acetylacetone and ammonia in aqueous solution to form α-α'-dimethyl-β-β'-diacetyl-pyridine which is excited at 400 nm and fluoresces at 510 nm). The Hantzsch reagents were prepared every three days and were kept cool in a refrigerator. A Teflon filter was installed at the sampling inlet to remove
30 particles from the air. This analyzer was calibrated with 1 μM HCHO standard solution every two to three days during the field measurements. The measurement uncertainty is ~20% and the detection limit is ~0.15 ppb (Hak et al., 2005).

4

2.1.4 GAC-IC measurements

Three semi-volatile gases (NH_3, HNO_3, and HCl) were measured with a time resolution of 30 min. The instrument was modified based on the Steam Jet Aerosol Collector (Khlystov et al., 1995) in order to better apply to the heavily polluted conditions in China (Dong et al., 2012). Gases were absorbed in a wet annular denuder and quantified by ion chromatography analyzers. Intercomparison experiments with filter sampling and other online methods showed that the relative uncertainties of GAC-IC were within ± 20% for major species (Song et al., 2018).

2.2 Approaches to estimating OS and methanesulfonate with HR-AMS

OS are primarily fragmented into separate organic ions ($C_xH_yO_z^+$) and inorganic sulfur-containing ions ($H_ySO_x^+$) with minimal organic sulfur-containing ions ($C_xH_yO_zS^+$), due to low thermal stability of OS and thermal vaporization and electron ionization of HR-AMS (Farmer et al., 2010; Huang et al., 2015; Hu et al., 2017a). The sulfate concentrations obtained by the standard HR-AMS data analysis are contributed not only by inorganic sulfate but also by OS. $(NH_4)_2SO_4$ is considered the dominant inorganic sulfate species in northern China winter haze aerosols due to the relatively high NH_3 levels and the resulting moderate particle acidity (Song et al., 2018). The presence of OS and its contribution to the HR-AMS sulfate (considered as the total sulfate) may be detectable using ratios between different $H_ySO_x^+$, due to different fragmentation patterns of $(NH_4)_2SO_4$ and OS (Hu et al., 2017a). For example, the major $H_ySO_x^+$ from $(NH_4)_2SO_4$ include S^+, SO^+, SO_2^+, SO_3^+, HSO_3^+, and $H_2SO_4^+$, while some of these (SO_3^+, HSO_3^+, and $H_2SO_4^+$) are not generated by HMS (Ge et al., 2012; Gilardoni et al., 2016). We observed in Beijing winter that the six ratios of $SO^+/H_ySO_x^+$ and $SO_2^+/H_ySO_x^+$ ($H_ySO_x^+$ refers to SO_3^+, HSO_3^+, and $H_2SO_4^+$) were highly correlated with each other ($r > 0.9$, $P < 0.001$), and that all of these ratios significantly increased with RH and PM_1 concentrations (Fig. 2a-b and Fig. S3). From the clean and dry conditions (average $PM_1 = 10$ µg m^{-3} and RH = 20%) to the haze (polluted and humid) conditions (average $PM_1 = 160$ µg m^{-3} and RH = 70%), these ion ratios increased by approximately 25–41%. During clean and dry periods, the observed ratios agreed well with values from pure $(NH_4)_2SO_4$ calibrations (Ge et al., 2012; Gilardoni et al., 2016; Hu et al., 2017a), supporting the dominance of $(NH_4)_2SO_4$ over other sulfur-containing compounds. The variations of $SO^+/H_ySO_x^+$ and $SO_2^+/H_ySO_x^+$ were unlikely due to changes in the acidity of haze aerosols (pH of about 4 to about 5 in both clean and haze conditions) (Song et al., 2018) and a clear relationship was not found between these fragment ratios and the fraction of ammonium nitrate in haze aerosols (Chen et al., 2018, Submitted). Examples are given in Fig. S4.

The enhancements of $SO^+/H_ySO_x^+$ and $SO_2^+/H_ySO_x^+$ under haze conditions may suggest the presence of additional sulfur compounds, which should either not generate SO_3^+, HSO_3^+, and $H_2SO_4^+$ ions or have higher ratios of $SO^+/H_ySO_x^+$ and $SO_2^+/H_ySO_x^+$ relative to $(NH_4)_2SO_4$. Since several types of OS (e.g., organosulfates and HMS) satisfy this requirement, the

5

observed HR-AMS mass spectra of inorganic sulfur-containing ions cannot be used to quantify the speciation of OS, but may allow an estimate of sulfate-equivalent OS concentration (C_{OS}, µg m^{-3})

$$C_{OS} = M_{SO_4^{2-}} \cdot \left[\left(SO_{obs}^+ - \overline{R_{cd,SO^+/H_ySO_x^+} \cdot H_ySO_{x,obs}^+} \right) / M_{SO^+} + \left(SO_{2,obs}^+ - \overline{R_{cd,SO_2^+/H_ySO_x^+} \cdot H_ySO_{x,obs}^+} \right) / M_{SO_2^+} \right] \quad (1)$$

where SO_{obs}^+, $SO_{2,obs}^+$, and $H_ySO_{x,obs}^+$ ($SO_{3,obs}^+$, $HSO_{3,obs}^+$, and $H_2SO_{4,obs}^+$) are concentrations of the observed inorganic sulfur-

5   containing ions, M_{SO^+}, $M_{SO_2^+}$, and $M_{SO_4^{2-}}$ are molar masses, and $R_{cd,SO^+/H_ySO_x^+}$ and $R_{cd,SO_2^+/H_ySO_x^+}$ indicate the average ratios of

the two corresponding ions observed during the clean and dry periods. $\overline{R_{cd,SO^+/H_ySO_x^+} \cdot H_ySO_{x,obs}^+}$ is considered to be the

concentration of SO$^+$ attributable to inorganic sulfate, and its difference from SO_{obs}^+ represents the contribution of OS. The

same applies to $\overline{R_{cd,SO_2^+/H_ySO_x^+} \cdot H_ySO_{x,obs}^+}$. This approach results in a conservative estimate of C_{OS} because (1) it is assumed that

OS do not generate SO_3^+, HSO_3^+, and $H_2SO_4^+$ ions; and (2) several minor ions (e.g., S$^+$ and $^{33}SO_2^+$) generated by OS

10   fragmentation are not taken into account (Hu et al., 2017b). The uncertainty quantification of C_{OS} is provided in Text S1.

The organic sulfur-containing ions $CH_3SO_2^+$ and $CH_2SO_2^+$ were used as the signature fragments of methanesulfonate (Ge et al., 2012). In our field measurements, an excellent linear correlation ($r = 0.98$, $P < 0.001$) was observed between these two ions and the average ratio of $CH_3SO_2^+$ to $CH_2SO_2^+$ (2.9 ± 0.1) was consistent with the value of 2.9 ± 0.3 from the HR-AMS mass

15   spectrum of pure MSA particles found in previous studies (Ge et al., 2012; Huang et al., 2015; Huang et al., 2017), confirming the presence of methanesulfonate in haze aerosols (Fig. S54). We estimated the levels of methanesulfonate using the observed $CH_3SO_2^+$ and its fraction in the total signal intensity of MSA standards identified in Huang et al. (2017).

2.3 WRF-Chem air quality model simulation

The Weather Research and Forecasting model coupled with Chemistry (WRF-Chem; version 3.5.1) (Grell et al., 2005) was

20   adopted to simulate concentrations of particulate sulfate and gas-phase HCHO during the 2014 winter (November–December). Two nested domains were configured to cover East Asia, and model results from the inner domain focused on northern China with a horizontal resolution of about 27 km were used for analysis. The meteorological initial and boundary conditions were obtained from the NCEP FNL (Final) Operational Global Analysis (NCEP, 2000), and temperature, moisture, and wind fields were nudged to constrain the accuracy of the simulated meteorology. The chemical initial and boundary conditions were

25   provided from MOZART-4 global model simulations of trace gases and aerosols (Emmons et al., 2010). The Lin microphysics scheme (Lin et al., 1983), Rapid Radiative Transfer Model (Mlawer et al., 1997), Goddard shortwave radiation scheme (Kim and Wang, 2011), Noah Land Surface Model (Chen and Dudhia, 2001), and YSU planetary boundary layer scheme (Hong et al., 2006) were used for the calculations of cloud microphysics, longwave radiation, shortwave radiation, land surface, and boundary layer processes, respectively. The Carbon Bond Mechanism version Z (CBM-Z) (Zaveri and Peters, 1999) gas-phase

30   chemical mechanism coupled with the thermodynamic module MOSAIC (Model for Simulating Aerosol Interactions and Chemistry) (Zaveri et al., 2008) was applied to simulate gas-phase reactions and aerosol processes.

Anthropogenic emissions were obtained from the MIX inventory (Li et al., 2017b) for five sectors, namely power generation, industry, residential, transportation, and agriculture, including the emissions of SO_2, NO_x, CO, non-methane volatile organic compounds (NMVOCs), NH_3, and primary inorganic and organic particulate matters. In addition, biogenic emissions were estimated using the Model of Emissions of Gases and Aerosols from Nature (MEGAN) (Guenther et al., 2006), and open biomass burning emissions were taken from the Global Fire Emissions Database version 4 (GFEDv4) (Randerson et al., 2017). In the WRF-Chem model, sulfate was formed by oxidation of SO_2 both in the gas phase (initiated by OH) and in cloud/fog water (by dissolved H_2O_2, O_3, and transition-metal-catalyzed O_2) (Pandis and Seinfeld, 1989)

$$SO_2 + OH + O_2 \rightarrow SO_3 + HO_2 \tag{2}$$

$$HSO_3^- + H_2O_2 \rightarrow SO_4^{2-} + H^+ + H_2O \tag{3}$$

$$SO_{2(aq)} + O_3 \rightarrow SO_4^{2-} + O_2 \tag{4}$$

$$SO_{2(aq)} + \tfrac{1}{2}O_2 \xrightarrow{Mn^{2+}, Fe^{3+}} SO_4^{2-} \tag{5}$$

where $SO_{2(aq)}$ represented the sum of $SO_2 \cdot H_2O$, HSO_3^-, and SO_3^{2-}.

We conducted two model simulations ~~(as described in Sect. 3.5)~~: (1) a BASE scenario with normal settings; (2) a 5×EMIS scenario in which primary HCHO emissions from the transportation sector was elevated by a factor of 5. This is because, as described in Sect. 3 (Results and discussion), the BASE scenario significantly underestimated ambient HCHO concentrations. It remains unclear whether primary or secondary sources of HCHO are responsible for its high wintertime levels. Jobson and colleagues have recently suggested that HCHO emissions during motor vehicle cold starts, especially in cold winter, are significantly underestimated in current inventories (Jobson et al., 2017). Accordingly, a 5×EMIS scenario with increasing primary HCHO emissions from transportation was conducted, which greatly reduces the negative biases in the modeled HCHO and thus was used to calculate the formation rate of HMS.

2.4 Apparent heterogeneous sulfate production rate

An apparent heterogeneous uptake of SO_2 on aerosols has been shown to be able to compensate for the missing sulfate (ΔSO_4^{2-}) in current air quality models during northern China winter haze episodes (Wang et al., 2014b; Zheng et al., 2015a; Li et al., 2018b). The heterogeneous sulfate production rate, P_Δ, was parameterized with an uptake coefficient γ (the fraction of gas-aerosol collisions resulting in chemical reaction) (Jacob, 2000)

$$P_\Delta = \left(R_p/D_g + 4/v\gamma\right)^{-1} S_p [SO_{2(g)}] M_{SO_4^{2-}} \tag{6}$$

where R_p is the average aerosol droplet radius taken as 0.15 μm following Cheng et al. (2016), D_g is the gas-phase diffusion coefficient of SO_2, v is the average molecular speed of SO_2, S_p is the aerosol surface area per unit volume of air, and $[SO_{2(g)}]$

7

is the gas-phase concentration. γ is 2×10^{-5} when RH $\leq 50\%$ and increases linearly from 2×10^{-5} to 5×10^{-5} when $50\% <$ RH $\leq 100\%$ (Zheng et al., 2015a), consistent with other laboratory and model studies (Wang et al., 2016; Li et al., 2017a). The heterogeneous reaction rate required to produce the identified OS (P_{OS}) can be expressed as

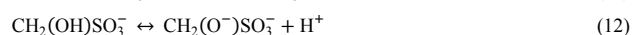$$P_{OS} = \left(C_{OS} / \Delta SO_4^{2-} \right) \cdot P_\Delta \qquad (7)$$

5 **2.5 ISORROPIA-II thermodynamic equilibrium model calculation**

We estimated AWC, aerosol water pH, and ionic strength with the ISORROPIA-II inorganic model (Fountoukis and Nenes, 2007) and also considered the contribution of carbonaceous species. Detailed calculations were given in our recent study (Song et al., 2018). Briefly, ISORROPIA-II predicts the phase partitioning of an NH_4^+–K^+–Ca^{2+}–Na^+–Mg^{2+}–SO_4^{2-}–NO_3^-–Cl^-–H_2O aerosol and semi-volatile gases (HNO_3, NH_3, and HCl), and can be used in either forward mode (the total (gas + aerosol)

10 concentration of each species is fixed) or reverse mode (the aerosol concentration of each species is fixed). The forward-mode results were adopted in this study, since the reverse-mode calculations of pH are sensitive to aerosol composition measurement errors and should be avoided. The model inputs were taken from the HR-AMS (bulk PM_1 composition) and GAC-IC (semi-volatile gas) measurements except for crustal species that were estimated based on their levels in $PM_{2.5}$ and typical size distributions (Song et al., 2018). The inorganic aerosol phase state was assumed to be metastable—meaning that the aqueous

15 solution does not crystallize but remains supersaturated when the RH is below the deliquescence RH, although aerosols may reside in a stable state—meaning that the aqueous solution crystallizes once saturation is exceeded (Rood et al., 1989). The assumed phase state led to a small difference in pH (<0.01 unit on average) and an average ~20% difference in AWC (Song et al., 2018), and thus did not affect the major conclusions of this study. The AWC modeled by ISORROPIA-II has been shown to be in good agreement with those based on ambient measurements in northern China (Wu et al., 2018). The validity of pH

20 calculations was supported by the reasonable agreement between the predicted and observed gas-particle partitioning of semi-volatile species (Song et al., 2018).

The aerosol water associated with carbonaceous species was estimated with the hygroscopicity parameter κ (Cheng et al., 2016). κ values of 0.06 and 0.04 were used for organics and black carbon, respectively (Song et al., 2018). Contribution of

25 carbonaceous species to AWC was found small (~10%), leading to a minor effect on pH (~0.05 unit). The ionic strength of aerosol water was estimated using the predicted aerosol composition and AWC (Herrmann, 2003). The uncertainty in pH was estimated with a Monte Carlo approach accounting for measurement errors in the model inputs including gas and aerosol species and meteorological parameters. The 95% confidence interval for calculated pH values was 4.1 to 5.5, very similar to the pH range found in previous northern China winter haze studies (Song et al., 2018).

30 **2.6 Kinetics and thermodynamics of HMS heterogeneous production**

The chemical mechanism for HMS production can be expressed as (Boyce and Hoffmann, 1984)

8

$$SO_2 \cdot H_2O \leftrightarrow HSO_3^- + H^+ \tag{8}$$

$$HSO_3^- \leftrightarrow SO_3^{2-} + H^+ \tag{9}$$

$$HCHO + HSO_3^- \overset{k_1}{\leftrightarrow} CH_2(OH)SO_3^- \tag{10}$$

$$HCHO + SO_3^{2-} \overset{k_2}{\leftrightarrow} CH_2(O^-)SO_3^- \tag{11}$$

$$CH_2(OH)SO_3^- \leftrightarrow CH_2(O^-)SO_3^- + H^+ \tag{12}$$

$$CH_2(OH)SO_3H \leftrightarrow CH_2(OH)SO_3^- + H^+ \tag{13}$$
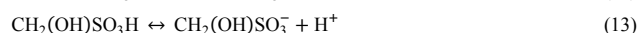
$CH_2(OH)SO_3H$ (hydroxymethanesulfonic acid, HMSA) dissociates twice to form $CH_2(OH)SO_3^-$ and $CH_2(O^-)SO_3^-$ with the dissociation constants $pK_{a1} < 0$ and $pK_{a2} \sim 12$, respectively, and thus, in the pH range of this study, the adduct existed as $CH_2(OH)SO_3^-$. The acid catalysis of HMS production was significant only at pH < 1 and thus irrelevant in the present context (Olson and Hoffmann, 1989). It is noted that $CH_2(OH)SO_3^-$ may form salts by the neutralization reaction with ammonium or other cations (e.g., Na^+, K^+, and Ca^{2+}) and undergo precipitation when the ambient RH becomes lower than the efflorescence RH value.

Production of HMS in aerosol water was found not limited by the mass transfer processes and hydration of HCHO (Text S2). The rate for heterogeneous production of HMS, P_{HMS} (in sulfate-equivalent µg m^{-3} h^{-1}), was calculated as

$$P_{HMS} = (k_1\alpha_1 + k_2\alpha_2) \cdot [SO_{2(aq)}] \cdot [HCHO_{(aq)}] \cdot AWC \cdot M_{SO_4^{2-}} \tag{14}$$

where k_1 and k_2 were, respectively, the forward rate constants for reactions (10) and (11), $[SO_{2(aq)}]$ (defined as the sum of $SO_2 \cdot H_2O$, HSO_3^-, and SO_3^{2-}) and $[HCHO_{(aq)}]$ were aqueous-phase concentrations estimated with their gas-phase levels and Henry's law constants. α_1 and α_2 represented the fractions of HSO_3^- and SO_3^{2-} in $SO_{2(aq)}$, respectively, and both were functions of pH. Production of HMS was reversible and the equilibrium constant K_{eq} could be expressed as

$$K_{eq} = [HMS_{(aq)}]/([HCHO_{(aq)}][SO_{2(aq)}]) \tag{15}$$

where $[HMS_{(aq)}]$ was the aqueous-phase concentration of HMS. Because the time to reach the equilibrium under winter haze conditions was typically greater than that for haze formation, the precursors and HMS were usually not equilibrated (Text S3). The relevant physical and chemical properties of SO_2, HCHO, and HMS are summarized in Tables S2 and S3.

3 Results and discussion

3.1 Presence of OS in Beijing winter haze aerosols

The standard HR-AMS data analysis usually does not distinguish OS from inorganic sulfate, since OS are fragmented primarily into separate organic ions and inorganic sulfur-containing ions (Hu et al., 2017a). Using the distinct fragmentation patterns of

9

inorganic sulfur-containing ions in the observed HR-AMS mass spectra, we derived a conservative estimate of total OS concentrations (expressed in sulfate-equivalent µg m^{-3}) in PM$_1$ (particles with an aerodynamic diameter below 1 µm), as described in Methods. During several winter haze periods (defined as PM$_1$ > 100 µg m^{-3}), OS were estimated to contribute significantly to the total sulfate (TS) identified by the standard HR-AMS data analysis, with an average OS/TS ratio of 17% ±
5 7% and a maximum ratio of 31% (Fig. 2a–b). Thus, previously reported sulfate concentrations in Beijing winter haze aerosols from HR-AMS measurements may have been biased high due to the presence of OS.

A good positive correlation ($r = 0.82$, $P < 0.001$) was found between OS and the AWC (Fig. 2c) estimated on the basis of the ISORROPIA-II thermodynamic equilibrium model constrained using in situ gas and aerosol compositional and meteorological
10 measurements (see Methods), suggesting that aerosol water serves as a medium enabling production of OS. It has been shown that PM$_1$ are in the liquid phase state during Beijing winter haze periods (Liu et al., 2017b). In contrast, OS were unrelated to the presence or absence of cloud/fog events (Fig. S65), indicating that the identified OS were less likely formed by local cloud/fog processing (Moch et al., 2018). Although our interpretation of the HR-AMS fragmentation of inorganic sulfur-containing ions cannot directly determine the speciation of OS (organosulfates, sulfones, methanesulfonate, and
15 hydroxyalkylsulfonates), we suggest, through the following analyses, that HMS may be the major OS species in Beijing winter haze aerosols.

3.2 Methanesulfonate, sulfones, and organosulfates are likely minor OS species

Contribution of methanesulfonate to OS was only 2%–8% estimated using CH$_3$SO$_2^+$ as the characteristic fragment in the HR-AMS mass spectra (see Methods and Fig. S4S5) (Huang et al., 2017). Its estimated concentrations were comparable to those
20 from a previous study (Yuan et al., 2004). The methanesulfonate in Beijing winter is likely formed by oxidation of dimethyl sulfite or dimethyl sulfoxide emitted from waste disposal (Yuan et al., 2004). Aerosol water has been suggested to play important roles in the formation of methanesulfonate and its condensation onto particles (Barnes et al., 2006; Gaston et al., 2010).

25 Formation of bis-hydroxymethyl sulfone (C$_2$H$_6$SO$_4$), the only sulfone that has been identified in ambient aerosols, is inhibited by atmospheric water and is thus unlikely to be important in winter haze (Eatough and Hansen, 1984). Organosulfates, formed through reactions of gaseous organics (e.g., epoxides and aldehydes) and particulate inorganic sulfate, also seem to represent minor contributions to OS based on the following evidence. The most common organosulfates identified previously in ambient aerosols, such as glycolic acid sulfate (C$_2$H$_3$SO$_6^-$), 2-methylglyceric acid sulfate (C$_4$H$_7$SO$_7^-$), isoprene epoxydiols sulfate
30 (C$_5$H$_{11}$SO$_7^-$), and benzyl (or methyl phenyl) sulfate (C$_7$H$_7$SO$_4^-$) (Froyd et al., 2010; Hatch et al., 2011a; Ma et al., 2014), were not detected by SPAMS measurements taken in Beijing winter. Production of organosulfates is enhanced by increased aerosol acidity (Surratt et al., 2010; Hatch et al., 2011b; Riva et al., 2016), whereas the relatively high pH values of about 4 to about 5 for winter haze aerosols in northern China may represent a limiting factor (Song et al., 2018).

10

3.3 HMS is likely the major OS species

Since the only known source of HMS ($CH_2(OH)SO_3^-$) is the nucleophilic addition of HSO_3^- and SO_3^{2-} to HCHO in aqueous solutions (Boyce and Hoffmann, 1984) (Fig. 3a; see Methods), the dominance of HMS in OS can explain the excellent correlation found between OS and AWC (Fig. 2c). The other hydroxyalkylsulfonate species are estimated to be less important than HMS, according to the laboratory experimental data from Hoffmann and colleagues (Olson and Hoffmann, 1989) and the abundance of different aldehydes in the atmosphere (Text S3).

Mass concentrations of HMS have been observed to be low, on the order of 0.01 μg m^{-3}, during several field campaigns in the United States, Germany, and Japan (Dixon and Aasen, 1999; Suzuki et al., 2001; Scheinhardt et al., 2014). However, heterogeneous production of HMS can be fast during winter haze periods in northern China because of moderately acidic pH of aerosol water, high AWC, high precursor (SO_2 and HCHO) concentrations, and low temperature. First, laboratory experiments have indicated that HMS production rates increase rapidly with pH, responding mainly to the dependence of SO_3^{2-} (a more efficient nucleophile than HSO_3^-) on pH (Boyce and Hoffmann, 1984; Kok et al., 1986). Values of aerosol water pH of about 4 to 5 obtained during the NCP winter haze events (Song et al., 2018) are 2 to 3 units higher than typically found in North America and Europe (Guo et al., 2017a), implying a factor of >10^4 enhancement in HMS production rates. Second, the AWC during winter haze periods (on the order of 100 μg m^{-3}) is among the highest in the world (Nguyen et al., 2016), providing a reactor to facilitate for aqueous reactions. Third, concentrations of both precursor gases are relatively high. Gaseous HCHO has been measured to be about 6 ppb on average in Beijing winter and increases on haze days (Rao et al., 2016). Although emissions of SO_2 have rapidly declined, especially since implementation of the National Air Pollution Prevention and Control Action Plan in 2013, its concentrations in the NCP remain much higher than in many other parts of the world (Shao et al., 2018). Last, low temperature in winter increases the solubility of precursor gases in water (Sander, 2015) and thus enhances HMS production rates. The reaction rate constants for HMS production decrease at low temperature but to a less extent (Boyce and Hoffmann, 1984).

In order to evaluate whether HMS production was fast enough to account for the identified OS, we calculated the rate for HMS production in aerosol water (P_{HMS}), and compared this with the apparent heterogeneous reaction rate that would be required to produce the identified OS (P_{OS}). As described in Methods, P_{HMS} calculations involved concentrations of gaseous SO_2 and HCHO (Fig. 3c), Henry's law constants, AWC and pH (95% confidence interval: 4.1–5.5), and reaction rate constants from laboratory experiments. HCHO concentrations simulated by the WRF-Chem air quality model (5×EMIS scenario; see Methods and Sect. 3.5) were used because its measurements were available only in December. The modeled HCHO was well correlated with its measured values ($r = 0.8$, $P < 0.001$), but was biased low by ~20% (Fig. 4). P_{HMS} was most sensitive to particle acidity and increased rapidly with pH, becoming comparable to P_{OS} when using the upper limit of pH (5.5) (Fig. 3d). P_{HMS} calculated here was expected to be conservative. Henry's law constants and kinetic data were obtained in relatively dilute solutions, while

11

aerosol water constitutes a concentrated electrolyte solution. The high ionic strength of aerosol water (~11 M during haze periods) may strongly increase formaldehyde solubility (Toda et al., 2014) and may further enhance kinetic rates for HMS production (Text S4). Gaseous HCHO concentrations used in the calculations were also biased low. It is very likely that the actual P_{HMS} was comparable to P_{OS} at a pH below 5.5, within the uncertainty range of calculated aerosol water pH. Note that

5   production of HMS was a minor sink of HCHO because the corresponding lifetime of ~4 days was greater than that against photolysis and oxidation by OH (~1 day in Beijing winter).

Our field measurements with SPAMS confirmed the existence of HMS in winter haze aerosols (Fig. 3b). Individual particles containing HMS were identified by the characteristic mass-to-charge ratio m/z −111 ($CH_2(OH)SO_3^-$) in the SPAMS mass

10   spectra (Whiteaker and Prather, 2003). The observed number concentration of HMS-containing particles (N_{HMS}) was closely correlated with AWC ($r = 0.86$, $P < 0.001$), supporting the production of HMS in aerosol droplets. A good relationship was also found between N_{HMS} and the identified OS from HR-AMS (Fig. 3b). Although the SPAMS data showed a significant percentage (~10% during haze periods) of HMS-containing particles in the total particle counts, a quantitative estimate of HMS mass concentration is not available here because HMS may be fragmented into smaller ions, such as HSO_3^- and SO_3^-,

15   depending on the countercations in particles (i.e., matrix effects) (Neubauer et al., 1997; Whiteaker and Prather, 2003). These ions coexist with the HMS peak in the SPAMS mass spectra (Fig. S6S7).

3.4 Implications of heterogeneous HMS chemistry

We have shown above in Beijing winter haze aerosols that a significant fraction of the missing sulfate based on HR-AMS measurements may be attributed to OS, which likely exist primarily as HMS and are misidentified as inorganic sulfate by the

20   standard HR-AMS data analysis. If HMS is assumed to represent the only OS compound, we estimated that it may account for about 1/3 of the missing sulfate in Beijing winter haze aerosols (Fig. S7S8). Interestingly, HMS would also likely be misidentified as inorganic sulfate (SO_4^{2-}) with typical ion chromatography (IC) analysis, another common method used to determine aerosol chemical compositions. In fact, nearly all of the particulate sulfate measurements in northern China winter haze have been made using these two techniques (He et al., 2014; Cheng et al., 2016; Wang et al., 2016; Li et al., 2017a; He

25   et al., 2018). For anion detection in IC, pH of the carrier fluid (known as eluent, a solution of KOH, NaOH, NaHCO$_3$, etc.) is usually greater than 9 (Wang et al., 2005; Cao et al., 2012; Liu et al., 2016; Han et al., 2017). HMS is unstable under such an alkaline environment and dissociates rapidly into SO_3^{2-} and HCHO (Seinfeld and Pandis, 2016)

$$CH_2(OH)SO_3^- + OH^- \rightarrow HCHO + SO_3^{2-} + H_2O \qquad (16)$$
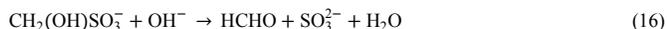
The characteristic time for HMS dissociation at pH > 9 is less than 1 minute (Seinfeld and Pandis, 2016), much less than the

30   retention time of SO_4^{2-}. The product SO_3^{2-} can be rapidly oxidized to SO_4^{2-} by oxidants (e.g., O$_3$ and H$_2$O$_2$) either generated or dissolved in aqueous extracts.

12

As described in Sect. 2.6, HMS should exist as the $CH_2(OH)SO_3^-$ anion in wet aerosols and may form salts with ammonium or other cations when aerosol particles dry out. A possible fate of HMS is to be oxidized by aqueous OH radicals producing peroxysulfate radicals ($SO_5^{\bullet-}$) (HMS is resistant to H_2O_2 and O_3) (Olson and Fessenden, 1992)

More intriguingly, heterogeneous HMS chemistry can provide an additional reaction pathway for inorganic sulfate production. Although being resistant to H_2O_2 and O_3, HMS is oxidized by aqueous OH radicals producing peroxysulfate radicals ($SO_5^{\bullet-}$) (Olson and Fessenden, 1992)
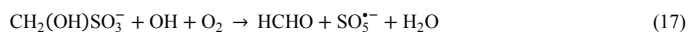
$$CH_2(OH)SO_3^- + OH + O_2 \rightarrow HCHO + SO_5^{\bullet-} + H_2O \qquad (17)$$

$SO_5^{\bullet-}$ is an intermediate in the free-radical chain reactions oxidizing SO_2 to SO_4^{2-}, and for each attack of OH on HMS, multiple SO_4^{2-} ions are produced (Fig. S8S9). Importantly, a HCHO molecule is released by reaction (17), suggesting that this reaction pathway does not result in net consumption of HCHO and that HMS serves as a temporary reservoir of tetravalent sulfur. We speculate from the diurnal patterns of HMS production rates (P_{HMS}) and the identified OS concentrations that oxidation of HMS by OH is likely to occur during daytime (Tan et al., 2018). (Fig. S8S9). But the rate of reaction (17) should be relatively slow when compared with that of reactions (10–11) because a significant level of HMS is expected to reside in the haze aerosol particles. A quantitative rate estimation for this pathway, however, is difficult, because aqueous OH is short-lived and it can be derived as a result of uptake from the gas phase or be generated or scavenged in the condensed phase (Jacob, 1986; Ervens et al., 2014). It is noted that the gaseous OH levels have been reported to remain relatively high during winter haze periods (Tan et al., 2018).

3.5 Future research needs

This study points to a potentially important role of heterogeneous HMS chemistry in explaining the missing sulfate problem during Beijing winter haze episodes. HMS has also been suggested to promote new particle formation by stabilizing sulfuric acid clusters (Li et al., 2018a). Although our field measurements and data interpretation focus on Beijing, this chemical mechanism should be important throughout the NCP because winter haze pollution is regional, as indicated by the distribution of SO_2 and HCHO (Fig. S109). Different from many other proposed pathways for sulfate production, HMS chemistry has a characteristic reaction product. More accurate quantification of HMS (e.g., using capillary electrophoresis and ion pairing chromatography (Munger et al., 1986; Scheinhardt et al., 2014)) in future field studies is essential to improve our understanding of this mechanism. In addition, three-dimensional chemical transport model studies should be conducted to further explore the HMS formation pathways and the associated uncertainties (e.g., pH values). The modeling simulations may also demonstrate whether significant amount of HMS can be formed in cloud droplets before transported to the ground level (Eck et al., 2012; Li et al., 2014).

This study reveals the unappreciated role of HCHO in Chinese haze through forming the complex HMS with SO_2, and it should be noted that HCHO also serves as a critical source of HO_x (OH + HO_2) radicals by photolysis (Rao et al., 2016) and as a

13

carcinogen (Zhu et al., 2017). In spite of its importance, our knowledge of the sources and chemical processes of HCHO during northern China winter haze events remains limited. ~~Further research should be conducted to elucidate HCHO sources in northern China winter and to design targeted mitigation measures.~~

~~The standard WRF-Chem model (BASE scenario) underestimated HCHO with a normalized mean bias of −67% (Fig. 4). It is~~
5   ~~unclear whether primary or secondary sources of HCHO are responsible for its high wintertime levels. Jobson and colleagues have recently suggested that HCHO emissions during motor vehicle cold starts, especially in cold winter, are significantly underestimated in current inventories (Jobson et al., 2017). Accordingly, we conduct a WRF-Chem sensitivity simulation (5×EMIS scenario), which increases primary HCHO emissions from transportation by a factor of 4 and greatly reduces the negative biases in the modeled HCHO (Fig. 4). However, further research should be conducted to elucidate HCHO sources in~~
10   ~~northern China winter and to design targeted mitigation measures.~~

4 Summary

Combing field measurements and model calculations, we propose a potentially important chemical mechanism, heterogeneous HMS chemistry, for secondary aerosol formation during northern China winter haze episodes. This mechanism involves the production of HMS by HCHO and SO_2 in aerosol water, which is favored under northern China winter haze conditions due to
15   several factors including high aerosol water content, moderately acidic pH, high gaseous precursor levels, and low temperature. ~~The produced HMS may be further oxidized to inorganic sulfate through a chain reaction in the presence of aqueous OH in aerosol water.~~ More field, laboratory, and modeling studies are needed in order to elucidate this chemical mechanism and to better understand the emission sources and atmospheric chemical processes impacting HCHO under winter haze conditions.

Data availability

20   All data supporting this study are available in this article and its Supplement, or from the corresponding authors upon request.

References

Bahreini, R., Ervens, B., Middlebrook, A. M., Warneke, C., de Gouw, J. A., DeCarlo, P. F., Jimenez, J. L., Brock, C. A., Neuman, J. A., Ryerson, T. B., Stark, H., Atlas, E., Brioude, J., Fried, A., Holloway, J. S., Peischl, J., Richter, D., Walega, J., Weibring, P., Wollny, A. G., and Fehsenfeld, F. C.: Organic aerosol formation in urban and industrial plumes near Houston
5   and Dallas, Texas, J. Geophys. Res. Atmos., 114, D00F16, doi:10.1029/2008JD011493, 2009.

Barnes, I., Hjorth, J., and Mihalopoulos, N.: Dimethyl sulfide and dimethyl sulfoxide and their oxidation in the atmosphere, Chem. Rev., 106, 940-975, doi:10.1021/cr020529+, 2006.

Boyce, S. D., and Hoffmann, M. R.: Kinetics and mechanism of the formation of hydroxymethanesulfonic acid at low pH, J. Phys. Chem., 88, 4740-4746, doi:10.1021/j150664a059, 1984.

10   Cai, W., Li, K., Liao, H., Wang, H., and Wu, L.: Weather conditions conducive to Beijing severe haze more frequent under climate change, Nat. Clim. Change., 7, 257-262, doi:10.1038/nclimate3249, 2017.

Cao, J., Wang, Q., Chow, J. C., Watson, J. G., Tie, X., Shen, Z., Wang, P., and An, Z.: Impacts of aerosol compositions on visibility impairment in Xi'an, China, Atmos. Environ., 59, 559-566, doi:10.1016/j.atmosenv.2012.05.036, 2012.

Charlson, R. J., Schwartz, S. E., Hales, J. M., Cess, R. D., Coakley, J. A., Hansen, J. E., and Hoffmann, D. J.: Climate forcing
15   by anthropogenic aerosols, Science, 255, 423-430, doi:10.1126/science.255.5043.423, 1992.

Chen, F., and Dudhia, J.: Coupling an advanced land surface–hydrology model with the Penn State–NCAR MM5 modeling system. part I: model implementation and sensitivity, Mon. Wea. Rev., 129, 569-585, doi:10.1175/1520-0493(2001)129<0569:caalsh>2.0.co;2, 2001.

Chen, Y., Xu, L., Humphry, T., Hettiyadura, A., Ovadnevaite, J., Huang, S., Poulain, L., Campuzano-Jost, P., Schroder, J.,
20   Jimenez, J., Herrmann, H., O'Dowd, C., Stone, E., and Ng, N. L.: Response of the Aerodyne Aerosol Mass Spectrometer to inorganic sulfates and organosulfur compounds: applications in field and laboratory measurements, Environ. Sci. Technol., 2018, Submitted.

Cheng, Y., Zheng, G., Wei, C., Mu, Q., Zheng, B., Wang, Z., Gao, M., Zhang, Q., He, K., Carmichael, G., Pöschl, U., and Su, H.: Reactive nitrogen chemistry in aerosol water as a source of sulfate during haze events in China, Sci. Adv., 2, e1601530,
25   doi:10.1126/sciadv.1601530, 2016.

Dall'Osto, M., Harrison, R. M., Coe, H., and Williams, P.: Real-time secondary aerosol formation during a fog event in London, Atmos. Chem. Phys., 9, 2459-2469, doi:10.5194/acp-9-2459-2009, 2009.

DeCarlo, P. F., Kimmel, J. R., Trimborn, A., Northway, M. J., Jayne, J. T., Aiken, A. C., Gonin, M., Fuhrer, K., Horvath, T., Docherty, K. S., Worsnop, D. R., and Jimenez, J. L.: Field-deployable, high-resolution, time-of-flight aerosol mass
30   spectrometer, Anal. Chem., 78, 8281-8289, doi:10.1021/ac061249n, 2006.

Ding, A. J., Huang, X., Nie, W., Sun, J. N., Kerminen, V.-M., Petäjä, T., Su, H., Cheng, Y. F., Yang, X.-Q., Wang, M. H., Chi, X. G., Wang, J. P., Virkkula, A., Guo, W. D., Yuan, J., Wang, S. Y., Zhang, R. J., Wu, Y. F., Song, Y., Zhu, T., Zilitinkevich,

S., Kulmala, M., and Fu, C. B.: Enhanced haze pollution by black carbon in megacities in China, Geophys. Res. Lett., 43, 2873-2879, doi:10.1002/2016GL067745, 2016.

Dixon, R. W., and Aasen, H.: Measurement of hydroxymethanesulfonate in atmospheric aerosols, Atmos. Environ., 33, 2023-2029, doi:10.1016/S1352-2310(98)00416-6, 1999.

5 Dong, H. B., Zeng, L. M., Hu, M., Wu, Y. S., Zhang, Y. H., Slanina, J., Zheng, M., Wang, Z. F., and Jansen, R.: Technical Note: The application of an improved gas and aerosol collector for ambient air pollutants in China, Atmos. Chem. Phys., 12, 10519-10533, doi:10.5194/acp-12-10519-2012, 2012.

Eatough, D. J., and Hansen, L. D.: Bis-hydroxymethyl sulfone: a major aerosol product of atmospheric reactions of $SO_2(g)$, Sci. Total Environ., 36, 319-328, doi:10.1016/0048-9697(84)90283-3, 1984.

10 Eck, T. F., Holben, B. N., Reid, J. S., Giles, D. M., Rivas, M. A., Singh, R. P., Tripathi, S. N., Bruegge, C. J., Platnick, S., Arnold, G. T., Krotkov, N. A., Carn, S. A., Sinyuk, A., Dubovik, O., Arola, A., Schafer, J. S., Artaxo, P., Smirnov, A., Chen, H., and Goloub, P.: Fog- and cloud-induced aerosol modification observed by the Aerosol Robotic Network (AERONET), J. Geophys. Res. Atmos., 117, doi:10.1029/2011JD016839, 2012.

Emmons, L. K., Walters, S., Hess, P. G., Lamarque, J. F., Pfister, G. G., Fillmore, D., Granier, C., Guenther, A., Kinnison, D., 15 Laepple, T., Orlando, J., Tie, X., Tyndall, G., Wiedinmyer, C., Baughcum, S. L., and Kloster, S.: Description and evaluation of the Model for Ozone and Related chemical Tracers, version 4 (MOZART-4), Geosci. Model Dev., 3, 43-67, doi:10.5194/gmd-3-43-2010, 2010.

Ervens, B., Sorooshian, A., Lim, Y. B., and Turpin, B. J.: Key parameters controlling OH‐initiated formation of secondary organic aerosol in the aqueous phase (aqSOA), J. Geophys. Res. Atmos., 119, 3997-4016, doi:10.1002/2013JD021021, 2014.

20 Farmer, D. K., Matsunaga, A., Docherty, K. S., Surratt, J. D., Seinfeld, J. H., Ziemann, P. J., and Jimenez, J. L.: Response of an aerosol mass spectrometer to organonitrates and organosulfates and implications for atmospheric chemistry, Proc. Natl. Acad. Sci. U.S.A., 107, 6670-6675, doi:10.1073/pnas.0912340107, 2010.

Fountoukis, C., and Nenes, A.: ISORROPIA II: a computationally efficient thermodynamic equilibrium model for K^+–Ca^{2+}–Mg^{2+}–NH_4^+–Na^+–SO_4^{2-}–NO_3^-–Cl^-–H_2O aerosols, Atmos. Chem. Phys., 7, 4639-4659, doi:10.5194/acp-7-4639-2007, 2007.

25 Froyd, K. D., Murphy, S. M., Murphy, D. M., de Gouw, J. A., Eddingsaas, N. C., and Wennberg, P. O.: Contribution of isoprene-derived organosulfates to free tropospheric aerosol mass, Proc. Natl. Acad. Sci. U.S.A., 107, 21360-21365, doi:10.1073/pnas.1012561107, 2010.

Fu, H., and Chen, J.: Formation, features and controlling strategies of severe haze-fog pollutions in China, Sci. Total Environ., 578, 121-138, doi:10.1016/j.scitotenv.2016.10.201, 2017.

30 Gao, J., Woodward, A., Vardoulakis, S., Kovats, S., Wilkinson, P., Li, L., Xu, L., Li, J., Yang, J., Li, J., Cao, L., Liu, X., Wu, H., and Liu, Q.: Haze, public health and mitigation measures in China: a review of the current evidence for further policy response, Sci. Total Environ., 578, 148-157, doi:10.1016/j.scitotenv.2016.10.231, 2017.

Gaston, C. J., Pratt, K. A., Qin, X., and Prather, K. A.: Real-time detection and mixing state of methanesulfonate in single particles at an inland urban location during a phytoplankton bloom, Environ. Sci. Technol., 44, 1566-1572, doi:10.1021/es902069d, 2010.

Ge, X., Zhang, Q., Sun, Y., Ruehl, C. R., and Setyan, A.: Effect of aqueous-phase processing on aerosol chemistry and size
5 distributions in Fresno, California, during wintertime, Environ. Chem., 9, 221-235, doi:10.1071/EN11168, 2012.

Gilardoni, S., Massoli, P., Paglione, M., Giulianelli, L., Carbone, C., Rinaldi, M., Decesari, S., Sandrini, S., Costabile, F., Gobbi, G. P., Pietrogrande, M. C., Visentin, M., Scotto, F., Fuzzi, S., and Facchini, M. C.: Direct observation of aqueous secondary organic aerosol from biomass-burning emissions, Proc. Natl. Acad. Sci. U.S.A., 113, 10013-10018, doi:10.1073/pnas.1602212113, 2016.

10 Grell, G. A., Peckham, S. E., Schmitz, R., McKeen, S. A., Frost, G., Skamarock, W. C., and Eder, B.: Fully coupled "online" chemistry within the WRF model, Atmos. Environ., 39, 6957-6975, doi:10.1016/j.atmosenv.2005.04.027, 2005.

Guenther, A., Karl, T., Harley, P., Wiedinmyer, C., Palmer, P. I., and Geron, C.: Estimates of global terrestrial isoprene emissions using MEGAN (Model of Emissions of Gases and Aerosols from Nature), Atmos. Chem. Phys., 6, 3181-3210, doi:10.5194/acp-6-3181-2006, 2006.

15 Guo, H., Liu, J., Froyd, K. D., Roberts, J. M., Veres, P. R., Hayes, P. L., Jimenez, J. L., Nenes, A., and Weber, R. J.: Fine particle pH and gas–particle phase partitioning of inorganic species in Pasadena, California, during the 2010 CalNex campaign, Atmos. Chem. Phys., 17, 5703-5719, doi:10.5194/acp-17-5703-2017, 2017a.

Guo, H., Weber, R. J., and Nenes, A.: High levels of ammonia do not raise fine particle pH sufficiently to yield nitrogen oxide-dominated sulfate production, Sci. Rep., 7, 12109, doi:10.1038/s41598-017-11704-0, 2017b.

20 Guo, S., Hu, M., Zamora, M. L., Peng, J., Shang, D., Zheng, J., Du, Z., Wu, Z., Shao, M., Zeng, L., Molina, M. J., and Zhang, R.: Elucidating severe urban haze formation in China, Proc. Natl. Acad. Sci. U.S.A., 111, 17373-17378, doi:10.1073/pnas.1419604111, 2014.

Hak, C., Pundt, I., Trick, S., Kern, C., Platt, U., Dommen, J., Ordóñez, C., Prévôt, A. S. H., Junkermann, W., Astorga-Lloréns, C., Larsen, B. R., Mellqvist, J., Strandberg, A., Yu, Y., Galle, B., Kleffmann, J., Lörzer, J. C., Braathen, G. O., and Volkamer,
25 R.: Intercomparison of four different in-situ techniques for ambient formaldehyde measurements in urban air, Atmos. Chem. Phys., 5, 2881-2900, doi:10.5194/acp-5-2881-2005, 2005.

Han, X., Guo, Q., Strauss, H., Liu, C., Hu, J., Guo, Z., Wei, R., Peters, M., Tian, L., and Kong, J.: Multiple sulfur isotope constraints on sources and formation processes of sulfate in Beijing $PM_{2.5}$ aerosol, Environ. Sci. Technol., 51, 7794-7803, doi:10.1021/acs.est.7b00280, 2017.

30 Hatch, L. E., Creamean, J. M., Ault, A. P., Surratt, J. D., Chan, M. N., Seinfeld, J. H., Edgerton, E. S., Su, Y., and Prather, K. A.: Measurements of isoprene-derived organosulfates in ambient aerosols by aerosol time-of-flight mass spectrometry - part 1: single particle atmospheric observations in Atlanta, Environ. Sci. Technol., 45, 5105-5111, doi:10.1021/es103944a, 2011a.

17

Hatch, L. E., Creamean, J. M., Ault, A. P., Surratt, J. D., Chan, M. N., Seinfeld, J. H., Edgerton, E. S., Su, Y., and Prather, K. A.: Measurements of isoprene-derived organosulfates in ambient aerosols by aerosol time-of-flight mass spectrometry—part 2: temporal variability and formation mechanisms, Environ. Sci. Technol., 45, 8648-8655, doi:10.1021/es2011836, 2011b.

He, H., Wang, Y., Ma, Q., Ma, J., Chu, B., Ji, D., Tang, G., Liu, C., Zhang, H., and Hao, J.: Mineral dust and NO_x promote the conversion of SO_2 to sulfate in heavy pollution days, Sci. Rep., 4, 4172, doi:10.1038/srep04172, 2014.

He, P., Alexander, B., Geng, L., Chi, X., Fan, S., Zhan, H., Kang, H., Zheng, G., Cheng, Y., Su, H., Liu, C., and Xie, Z.: Isotopic constraints on heterogeneous sulfate production in Beijing haze, Atmos. Chem. Phys., 18, 5515-5528, doi:10.5194/acp-18-5515-2018, 2018.

Herrmann, H.: Kinetics of aqueous phase reactions relevant for atmospheric chemistry, Chem. Rev., 103, 4691-4716, doi:10.1021/cr020658q, 2003.

Hong, S.-Y., Noh, Y., and Dudhia, J.: A new vertical diffusion package with an explicit treatment of entrainment processes, Mon. Wea. Rev., 134, 2318-2341, doi:10.1175/mwr3199.1, 2006.

Hu, W., Campuzano-Jost, P., Day, D. A., Croteau, P., Canagaratna, M. R., Jayne, J. T., Worsnop, D. R., and Jimenez, J. L.: Evaluation of the new capture vaporizer for aerosol mass spectrometers (AMS) through field studies of inorganic species, Aerosol Sci. Technol., 51, 735-754, doi:10.1080/02786826.2017.1296104, 2017a.

Hu, W., Campuzano-Jost, P., Day, D. A., Croteau, P., Canagaratna, M. R., Jayne, J. T., Worsnop, D. R., and Jimenez, J. L.: Evaluation of the new capture vapourizer for aerosol mass spectrometers (AMS) through laboratory studies of inorganic species, Atmos. Meas. Tech., 10, 2897-2921, doi:10.5194/amt-10-2897-2017, 2017b.

Huang, D. D., Li, Y. J., Lee, B. P., and Chan, C. K.: Analysis of organic sulfur compounds in atmospheric aerosols at the HKUST supersite in Hong Kong using HR-ToF-AMS, Environ. Sci. Technol., 49, 3672-3679, doi:10.1021/es5056269, 2015.

Huang, R.-J., Zhang, Y., Bozzetti, C., Ho, K.-F., Cao, J.-J., Han, Y., Daellenbach, K. R., Slowik, J. G., Platt, S. M., Canonaco, F., Zotter, P., Wolf, R., Pieber, S. M., Bruns, E. A., Crippa, M., Ciarelli, G., Piazzalunga, A., Schwikowski, M., Abbaszade, G., Schnelle-Kreis, J., Zimmermann, R., An, Z., Szidat, S., Baltensperger, U., Haddad, I. E., and Prévôt, A. S. H.: High secondary aerosol contribution to particulate pollution during haze events in China, Nature, 514, 218-222, doi:10.1038/nature13774, 2014.

Huang, S., Poulain, L., van Pinxteren, D., van Pinxteren, M., Wu, Z., Herrmann, H., and Wiedensohler, A.: Latitudinal and seasonal distribution of particulate MSA over the Atlantic using a validated quantification method with HR-ToF-AMS, Environ. Sci. Technol., 51, 418-426, doi:10.1021/acs.est.6b03186, 2017.

Hung, H.-M., Hsu, M.-N., and Hoffmann, M. R.: Quantification of SO_2 oxidation on interfacial surfaces of acidic micro-droplets: implication for ambient sulfate formation, Environ. Sci. Technol., accepted, doi:10.1021/acs.est.8b01391, 2018.

Jacob, D. J.: Chemistry of OH in remote clouds and its role in the production of formic acid and peroxymonosulfate, J. Geophys. Res. Atmos., 91, 9807-9826, doi:10.1029/JD091iD09p09807, 1986.

Jacob, D. J.: Heterogeneous chemistry and tropospheric ozone, Atmos. Environ., 34, 2131-2159, doi:10.1016/S1352-2310(99)00462-8, 2000.

18

Jayne, J. T., Leard, D. C., Zhang, X., Davidovits, P., Smith, K. A., Kolb, C. E., and Worsnop, D. R.: Development of an aerosol mass spectrometer for size and composition analysis of submicron particles, Aerosol Sci. Technol., 33, 49-70, doi:10.1080/027868200410840, 2000.

Jobson, B. T., Huangfu, Y., and Vanderschelden, G. S.: High time resolution measurements of VOCs from vehicle cold starts: the air toxic cold start pulse (abstract A53B-2227), AGU Fall Meeting, New Orleans, LA, USA, 2017.

Khlystov, A., Wyers, G. P., and Slanina, J.: The steam-jet aerosol collector, Atmos. Environ., 29, 2229-2234, doi:10.1016/1352-2310(95)00180-7, 1995.

Kim, H.-J., and Wang, B.: Sensitivity of the WRF model simulation of the East Asian summer monsoon in 1993 to shortwave radiation schemes and ozone absorption, Asia-Pac. J. Atmos. Sci., 47, 167-180, doi:10.1007/s13143-011-0006-y, 2011.

Kok, G. L., Gitlin, S. N., and Lazrus, A. L.: Kinetics of the formation and decomposition of hydroxymethanesulfonate, J. Geophys. Res. Atmos., 91, 2801-2804, doi:10.1029/JD091iD02p02801, 1986.

Lee, S. H., Murphy, D. M., Thomson, D. S., and Middlebrook, A. M.: Nitrate and oxidized organic ions in single particle mass spectra during the 1999 Atlanta Supersite Project, J. Geophys. Res. Atmos., 108, doi:10.1029/2001JD001455, 2003.

Li, G., Bei, N., Cao, J., Huang, R., Wu, J., Feng, T., Wang, Y., Liu, S., Zhang, Q., Tie, X., and Molina, L. T.: A possible pathway for rapid growth of sulfate during haze days in China, Atmos. Chem. Phys., 17, 3301-3316, doi:10.5194/acp-17-3301-2017, 2017a.

Li, H., Zhang, X., Zhong, J., Liu, L., Zhang, H., Chen, F., Li, Z., Li, Q., and Ge, M.: The role of hydroxymethanesulfonic acid in the initial stage of new particle formation, Atmos. Environ., 189, 244-251, doi:10.1016/j.atmosenv.2018.07.003, 2018a.

Li, L., Huang, Z., Dong, J., Li, M., Gao, W., Nian, H., Fu, Z., Zhang, G., Bi, X., Cheng, P., and Zhou, Z.: Real time bipolar time-of-flight mass spectrometer for analyzing single aerosol particles, Int. J. Mass Spectrom., 303, 118-124, doi:10.1016/j.ijms.2011.01.017, 2011.

Li, L., Hoffmann, M. R., and Colussi, A. J.: Role of nitrogen dioxide in the production of sulfate during Chinese haze-aerosol episodes, Environ. Sci. Technol., 52, 2686-2693, doi:10.1021/acs.est.7b05222, 2018b.

Li, M., Zhang, Q., Kurokawa, J. I., Woo, J. H., He, K., Lu, Z., Ohara, T., Song, Y., Streets, D. G., Carmichael, G. R., Cheng, Y., Hong, C., Huo, H., Jiang, X., Kang, S., Liu, F., Su, H., and Zheng, B.: MIX: a mosaic Asian anthropogenic emission inventory under the international collaboration framework of the MICS-Asia and HTAP, Atmos. Chem. Phys., 17, 935-963, doi:10.5194/acp-17-935-2017, 2017b.

Li, Z., Eck, T., Zhang, Y., Zhang, Y., Li, D., Li, L., Xu, H., Hou, W., Lv, Y., Goloub, P., and Gu, X.: Observations of residual submicron fine aerosol particles related to cloud and fog processing during a major pollution event in Beijing, Atmos. Environ., 86, 187-192, doi:10.1016/j.atmosenv.2013.12.044, 2014.

Lin, Y.-L., Farley, R. D., and Orville, H. D.: Bulk Parameterization of the Snow Field in a Cloud Model, J. Climate Appl. Meteor., 22, 1065-1092, doi:10.1175/1520-0450(1983)022<1065:bpotsf>2.0.co;2, 1983.

Liu, M., Song, Y., Zhou, T., Xu, Z., Yan, C., Zheng, M., Wu, Z., Hu, M., Wu, Y., and Zhu, T.: Fine particle pH during severe haze episodes in northern China, Geophys. Res. Lett., 44, 5213-5221, doi:10.1002/2017GL073210, 2017a.

19

Liu, P., Zhang, C., Mu, Y., Liu, C., Xue, C., Ye, C., Liu, J., Zhang, Y., and Zhang, H.: The possible contribution of the periodic emissions from farmers' activities in the North China Plain to atmospheric water-soluble ions in Beijing, Atmos. Chem. Phys., 16, 10097-10109, doi:10.5194/acp-16-10097-2016, 2016.

Liu, Y., Wu, Z., Wang, Y., Xiao, Y., Gu, F., Zheng, J., Tan, T., Shang, D., Wu, Y., Zeng, L., Hu, M., Bateman, A. P., and
5   Martin, S. T.: Submicrometer particles are in the liquid state during heavy haze episodes in the urban atmosphere of Beijing, China, Environ. Sci. Technol. Lett., 4, 427-432, doi:10.1021/acs.estlett.7b00352, 2017b.

Ma, Y., Xu, X., Song, W., Geng, F., and Wang, L.: Seasonal and diurnal variations of particulate organosulfates in urban Shanghai, China, Atmos. Environ., 85, 152-160, doi:10.1016/j.atmosenv.2013.12.017, 2014.

Middlebrook, A. M., Bahreini, R., Jimenez, J. L., and Canagaratna, M. R.: Evaluation of composition-dependent collection
10   efficiencies for the Aerodyne aerosol mass spectrometer using field data, Aerosol Sci. Technol., 46, 258-271, doi:10.1080/02786826.2011.620041, 2012.

Mlawer, E. J., Taubman, S. J., Brown, P. D., Iacono, M. J., and Clough, S. A.: Radiative transfer for inhomogeneous atmospheres: RRTM, a validated correlated-k model for the longwave, J. Geophys. Res. Atmos., 102, 16663-16682, doi:10.1029/97JD00237, 1997.

15   Moch, J. M., Dovrou, E., Mickley, L. J., Keutsch, F. N., Cheng, Y., Jacob, D. J., Jiang, J., Li, M., Munger, J. W., Qiao, X., and Zhang, Q.: Contribution of Hydroxymethane Sulfonate to Ambient Particulate Matter: A Potential Explanation for High Particulate Sulfur During Severe Winter Haze in Beijing, Geophys. Res. Lett., 45, 11969-11979, doi:10.1029/2018GL079309, 2018.

Munger, J. W., Tiller, C., and Hoffmann, M. R.: Identification of hydroxymethanesulfonate in fog water, Science, 231, 247-
20   249, doi:10.1126/science.231.4735.247, 1986.

Neubauer, K. R., Johnston, M. V., and Wexler, A. S.: On-line analysis of aqueous aerosols by laser desorption ionization, Int. J. Mass Spectrom., 163, 29-37, doi:10.1016/S0168-1176(96)04534-X, 1997.

Nguyen, T. K. V., Zhang, Q., Jimenez, J. L., Pike, M., and Carlton, A. G.: Liquid water: ubiquitous contributor to aerosol mass, Environ. Sci. Technol. Lett., 3, 257-263, doi:10.1021/acs.estlett.6b00167, 2016.

25   Olson, T. M., and Hoffmann, M. R.: Hydroxyalkylsulfonate formation: Its role as a S(IV) reservoir in atmospheric water droplets, Atmos. Environ., 23, 985-997, doi:10.1016/0004-6981(89)90302-8, 1989.

Olson, T. M., and Fessenden, R. W.: Pulse radiolysis study of the reaction of hydroxyl radicals with methanesulfonate and hydroxymethanesulfonate, J. Phys. Chem., 96, 3317-3320, doi:10.1021/j100187a027, 1992.

Pandis, S. N., and Seinfeld, J. H.: Sensitivity analysis of a chemical mechanism for aqueous‐phase atmospheric chemistry, J.
30   Geophys. Res. Atmos., 94, 1105-1126, doi:10.1029/JD094iD01p01105, 1989.

Prather, K. A., Nordmeyer, T., and Salt, K.: Real-time characterization of individual aerosol particles using time-of-flight mass spectrometry, Anal. Chem., 66, 1403-1407, doi:10.1021/ac00081a007, 1994.

Qin, M., Chen, Z., Shen, H., Li, H., Wu, H., and Wang, Y.: Impacts of heterogeneous reactions to atmospheric peroxides: observations and budget analysis study, Atmos. Environ., 183, 144-153, doi:10.1016/j.atmosenv.2018.04.005, 2018.

Rao, Z., Chen, Z., Liang, H., Huang, L., and Huang, D.: Carbonyl compounds over urban Beijing: concentrations on haze and non-haze days and effects on radical chemistry, Atmos. Environ., 124, 207-216, doi:10.1016/j.atmosenv.2015.06.050, 2016.

Riva, M., Da Silva Barbosa, T., Lin, Y. H., Stone, E. A., Gold, A., and Surratt, J. D.: Chemical characterization of organosulfates in secondary organic aerosol derived from the photooxidation of alkanes, Atmos. Chem. Phys., 16, 11001-

5 11018, doi:10.5194/acp-16-11001-2016, 2016.

Rood, M. J., Shaw, M. A., Larson, T. V., and Covert, D. S.: Ubiquitous nature of ambient metastable aerosol, Nature, 337, 537-539, doi:10.1038/337537a0, 1989.

Sander, R.: Compilation of Henry's law constants (version 4.0) for water as solvent, Atmos. Chem. Phys., 15, 4399-4981, doi:10.5194/acp-15-4399-2015, 2015.

10 Scheinhardt, S., van Pinxteren, D., Müller, K., Spindler, G., and Herrmann, H.: Hydroxymethanesulfonic acid in size-segregated aerosol particles at nine sites in Germany, Atmos. Chem. Phys., 14, 4531-4538, doi:10.5194/acp-14-4531-2014, 2014.

Seinfeld, J. H., and Pandis, S. N.: Atmospheric chemistry and physics: from air pollution to climate change, Third ed., John Wiley & Sons, Inc., Hoboken, New Jersey, 2016.

15 Shao, P., Tian, H., Sun, Y., Liu, H., Wu, B., Liu, S., Liu, X., Wu, Y., Liang, W., Wang, Y., Gao, J., Xue, Y., Bai, X., Liu, W., Lin, S., and Hu, G.: Characterizing remarkable changes of severe haze events and chemical compositions in multi-size airborne particles (PM$_1$, PM$_{2.5}$ and PM$_{10}$) from January 2013 to 2016–2017 winter in Beijing, China, Atmos. Environ., 189, 133-144, doi:10.1016/j.atmosenv.2018.06.038, 2018.

Song, S., Gao, M., Xu, W., Shao, J., Shi, G., Wang, S., Wang, Y., Sun, Y., and McElroy, M. B.: Fine-particle pH for Beijing

20 winter haze as inferred from different thermodynamic equilibrium models, Atmos. Chem. Phys., 18, 7423-7438, doi:10.5194/acp-18-7423-2018, 2018.

Sorooshian, A., Crosbie, E., Maudlin, L. C., Youn, J. S., Wang, Z., Shingler, T., Ortega, A. M., Hersey, S., and Woods, R. K.: Surface and airborne measurements of organosulfur and methanesulfonate over the western United States and coastal areas, J. Geophys. Res. Atmos., 120, 8535-8548, doi:10.1002/2015JD023822, 2015.

25 Sueper and collaborators: ToF-AMS Analysis Software, available at : http://cires.colorado.edu/jimenez-group/ToFAMSResources/ToFSoftware/index.html, last accessed 05/18/2018., 2018.

Sun, Y., Wang, Z., Fu, P., Jiang, Q., Yang, T., Li, J., and Ge, X.: The impact of relative humidity on aerosol composition and evolution processes during wintertime in Beijing, China, Atmos. Environ., 77, 927-934, doi:10.1016/j.atmosenv.2013.06.019, 2013.

30 Sun, Y., Du, W., Fu, P., Wang, Q., Li, J., Ge, X., Zhang, Q., Zhu, C., Ren, L., Xu, W., Zhao, J., Han, T., Worsnop, D. R., and Wang, Z.: Primary and secondary aerosols in Beijing in winter: sources, variations and processes, Atmos. Chem. Phys., 16, 8309-8329, doi:10.5194/acp-16-8309-2016, 2016.

21

Surratt, J. D., Gómez-González, Y., Chan, A. W. H., Vermeylen, R., Shahgholi, M., Kleindienst, T. E., Edney, E. O., Offenberg, J. H., Lewandowski, M., Jaoui, M., Maenhaut, W., Claeys, M., Flagan, R. C., and Seinfeld, J. H.: Organosulfate formation in biogenic secondary organic aerosol, J. Phys. Chem. A, 112, 8345-8378, doi:10.1021/jp802310p, 2008.

Surratt, J. D., Chan, A. W. H., Eddingsaas, N. C., Chan, M., Loza, C. L., Kwan, A. J., Hersey, S. P., Flagan, R. C., Wennberg,
5   P. O., and Seinfeld, J. H.: Reactive intermediates revealed in secondary organic aerosol formation from isoprene, Proc. Natl. Acad. Sci. U.S.A., 107, 6640-6645, doi:10.1073/pnas.0911114107, 2010.

Suzuki, Y., Kawakami, M., and Akasaka, K.: 1H NMR application for characterizing water-soluble organic compounds in urban atmospheric particles, Environ. Sci. Technol., 35, 2656-2664, doi:10.1021/es001861a, 2001.

Tan, Z., Rohrer, F., Lu, K., Ma, X., Bohn, B., Broch, S., Dong, H., Fuchs, H., Gkatzelis, G. I., Hofzumahaus, A., Holland, F.,
10 Li, X., Liu, Y., Liu, Y., Novelli, A., Shao, M., Wang, H., Wu, Y., Zeng, L., Hu, M., Kiendler-Scharr, A., Wahner, A., and Zhang, Y.: Wintertime photochemistry in Beijing: observations of ROx radical concentrations in the North China Plain during the BEST-ONE campaign, Atmos. Chem. Phys., 18, 12391-12411, doi:10.5194/acp-18-12391-2018, 2018.

Tie, X., Huang, R.-J., Cao, J., Zhang, Q., Cheng, Y., Su, H., Chang, D., Pöschl, U., Hoffmann, T., Dusek, U., Li, G., Worsnop, D. R., and O'Dowd, C. D.: Severe pollution in China amplified by atmospheric moisture, Sci. Rep., 7, 15760,
15 doi:10.1038/s41598-017-15909-1, 2017.

Toda, K., Yunoki, S., Yanaga, A., Takeuchi, M., Ohira, S.-I., and Dasgupta, P. K.: Formaldehyde content of atmospheric aerosol, Environ. Sci. Technol., 48, 6636-6643, doi:10.1021/es500590e, 2014.

Tolocka, M. P., and Turpin, B.: Contribution of organosulfur compounds to organic aerosol mass, Environ. Sci. Technol., 46, 7978-7983, doi:10.1021/es300651v, 2012.

20 Wang, A. H., Zhang, S. Y., Wang, H., Gong, D. C., Zhang, S. Y., Song, W., Chen, D. H., Zhou, L., and Tian, B. G.: A preliminary study of organosulfates in atmospheric aerosols at Tian-jing-shan national air background monitoring station in Nanling Mountains, South China, China Environmental Science, 37, 1663-1669, 2017.

Wang, G., Zhang, R., Gomez, M. E., Yang, L., Levy Zamora, M., Hu, M., Lin, Y., Peng, J., Guo, S., Meng, J., Li, J., Cheng, C., Hu, T., Ren, Y., Wang, Y., Gao, J., Cao, J., An, Z., Zhou, W., Li, G., Wang, J., Tian, P., Marrero-Ortiz, W., Secrest, J., Du,
25 Z., Zheng, J., Shang, D., Zeng, L., Shao, M., Wang, W., Huang, Y., Wang, Y., Zhu, Y., Li, Y., Hu, J., Pan, B., Cai, L., Cheng, Y., Ji, Y., Zhang, F., Rosenfeld, D., Liss, P. S., Duce, R. A., Kolb, C. E., and Molina, M. J.: Persistent sulfate formation from London Fog to Chinese haze, Proc. Natl. Acad. Sci. U.S.A., 113, 13630-13635, doi:10.1073/pnas.1616540113, 2016.

Wang, G., Zhang, F., Peng, J., Duan, L., Ji, Y., Marrero-Ortiz, W., Wang, J., Li, J., Wu, C., Cao, C., Wang, Y., Zheng, J., Secrest, J., Li, Y., Wang, Y., Li, H., Li, N., and Zhang, R.: Particle acidity and sulfate production during severe haze events in
30 China cannot be reliably inferred by assuming a mixture of inorganic salts, Atmos. Chem. Phys., 18, 10123-10132, doi:10.5194/acp-18-10123-2018, 2018.

Wang, J., Wang, S., Jiang, J., Ding, A., Zheng, M., Zhao, B., Wong, D. C., Zhou, W., Zheng, G., Wang, L., Pleim, J. E., and Hao, J.: Impact of aerosol–meteorology interactions on fine particle pollution during China's severe haze episode in January 2013, Environ. Res. Lett., 9, 094002, doi:10.1088/1748-9326/9/9/094002, 2014a.

22

Wang, Y., Zhuang, G., Tang, A., Yuan, H., Sun, Y., Chen, S., and Zheng, A.: The ion chemistry and the source of $PM_{2.5}$ aerosol in Beijing, Atmos. Environ., 39, 3771-3784, doi:10.1016/j.atmosenv.2005.03.013, 2005.

Wang, Y., Zhang, Q., Jiang, J., Zhou, W., Wang, B., He, K., Duan, F., Zhang, Q., Philip, S., and Xie, Y.: Enhanced sulfate formation during China's severe winter haze episode in January 2013 missing from current models, J. Geophys. Res. Atmos.,

5   119, 10425-10440, doi:10.1002/2013JD021426, 2014b.

Whiteaker, J. R., and Prather, K. A.: Hydroxymethanesulfonate as a tracer for fog processing of individual aerosol particles, Atmos. Environ., 37, 1033-1043, doi:10.1016/S1352-2310(02)01029-4, 2003.

Wu, Z., Wang, Y., Tan, T., Zhu, Y., Li, M., Shang, D., Wang, H., Lu, K., Guo, S., Zeng, L., and Zhang, Y.: Aerosol liquid water driven by anthropogenic inorganic salts: implying its key role in haze formation over the North China Plain, Environ.

10   Sci. Technol. Lett., 5, 160-166, doi:10.1021/acs.estlett.8b00021, 2018.

Xie, Y., Ding, A., Nie, W., Mao, H., Qi, X., Huang, X., Xu, Z., Kerminen, V.-M., Petäjä, T., Chi, X., Virkkula, A., Boy, M., Xue, L., Guo, J., Sun, J., Yang, X., Kulmala, M., and Fu, C.: Enhanced sulfate formation by nitrogen dioxide: Implications from in situ observations at the SORPES station, J. Geophys. Res. Atmos., 120, 12679-12694, doi:10.1002/2015JD023607, 2015.

15   Yu, T., Zhao, D., Song, X., and Zhu, T.: NO_2-initiated multiphase oxidation of SO_2 by O_2 on $CaCO_3$ particles, Atmos. Chem. Phys., 18, 6679-6689, doi:10.5194/acp-18-6679-2018, 2018.

Yuan, H., Wang, Y., and Zhuang, G.: MSA in Beijing aerosol, Sci. Bull., 49, 1020-1025, doi:10.1007/bf03184031, 2004.

Zaveri, R. A., and Peters, L. K.: A new lumped structure photochemical mechanism for large-scale applications, J. Geophys. Res. Atmos., 104, 30387-30415, doi:10.1029/1999JD900876, 1999.

20   Zaveri, R. A., Easter, R. C., Fast, J. D., and Peters, L. K.: Model for Simulating Aerosol Interactions and Chemistry (MOSAIC), J. Geophys. Res. Atmos., 113, D13204, doi:10.1029/2007JD008782, 2008.

Zhang, G., Bi, X., Chan, L. Y., Li, L., Wang, X., Feng, J., Sheng, G., Fu, J., Li, M., and Zhou, Z.: Enhanced trimethylamine-containing particles during fog events detected by single particle aerosol mass spectrometry in urban Guangzhou, China, Atmos. Environ., 55, 121-126, doi:10.1016/j.atmosenv.2012.03.038, 2012.

25   Zhao, D., Song, X., Zhu, T., Zhang, Z., Liu, Y., and Shang, J.: Multiphase oxidation of SO_2 by NO_2 on $CaCO_3$ particles, Atmos. Chem. Phys., 18, 2481-2493, doi:10.5194/acp-18-2481-2018, 2018.

Zheng, B., Zhang, Q., Zhang, Y., He, K. B., Wang, K., Zheng, G. J., Duan, F. K., Ma, Y. L., and Kimoto, T.: Heterogeneous chemistry: a mechanism missing in current models to explain secondary inorganic aerosol formation during the January 2013 haze episode in North China, Atmos. Chem. Phys., 15, 2031-2049, doi:10.5194/acp-15-2031-2015, 2015a.

30   Zheng, G. J., Duan, F. K., Su, H., Ma, Y. L., Cheng, Y., Zheng, B., Zhang, Q., Huang, T., Kimoto, T., Chang, D., Pöschl, U., Cheng, Y. F., and He, K. B.: Exploring the severe winter haze in Beijing: the impact of synoptic weather, regional transport and heterogeneous reactions, Atmos. Chem. Phys., 15, 2969-2983, doi:10.5194/acp-15-2969-2015, 2015b.

Zhu, L., Jacob, D. J., Keutsch, F. N., Mickley, L. J., Scheffe, R., Strum, M., González Abad, G., Chance, K., Yang, K., Rappenglück, B., Millet, D. B., Baasandorj, M., Jaeglé, L., and Shah, V.: Formaldehyde (HCHO) as a hazardous air pollutant:

mapping surface air concentrations from satellite and inferring cancer risks in the United States, Environ. Sci. Technol., 51, 5650-5657, doi:10.1021/acs.est.7b01356, 2017.
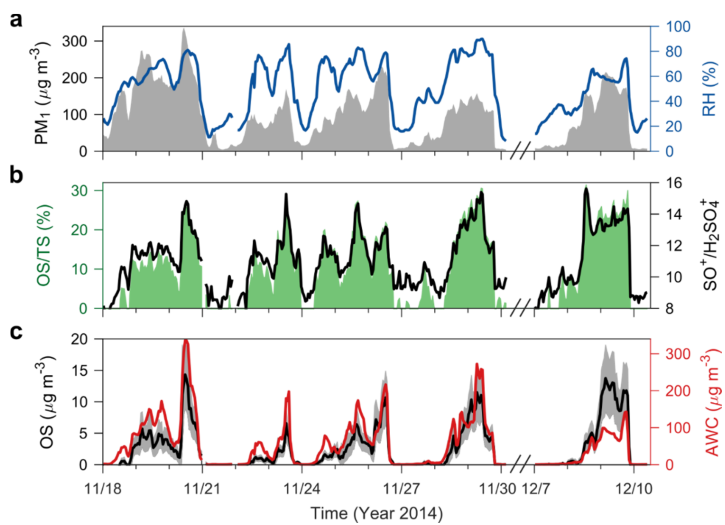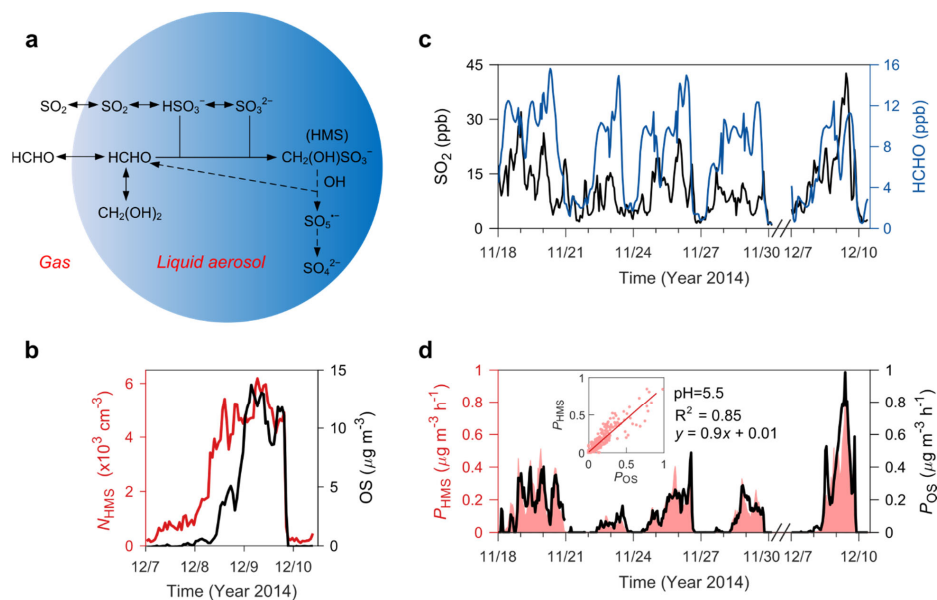
Figures
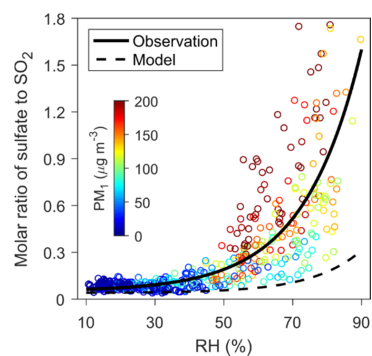
5

Figure 1. Relationship between sulfate/SO₂ molar ratio and RH. The circles indicate hourly observations during 2014 winter in urban Beijing, and are colored according to the observed PM_1 (particles with diameter less than 1 μm) concentrations. The solid and dashed curves represent, respectively, the exponential fitting between the observed and modeled sulfate/SO₂ ratios and the observed RH, i.e., $y = 0.05 + 7 \times 10^{-3} e^{0.06x}$ ($R^2 = 0.6$) and $y = 0.04 + 5 \times 10^{-4} e^{0.07x}$ ($R^2 = 0.3$). Sulfate concentrations are obtained from HR-AMS PM_1 measurements and
10 the corresponding model results are from WRF-Chem simulations.

Figure 2. Possible presence of OS in Beijing winter haze aerosols. (a) PM$_1$ concentrations (left, grey-shaded area) and RH (right, blue line). **(b)** Contributions of OS to TS (left, green-shaded area) and ratios of SO$^+$ to H$_2$SO$_4^+$ (right, black line). The ratios between the other inorganic sulfur-containing ions are given in Fig. S3. **(c)** Sulfate-equivalent OS concentrations (left, black line) and AWC (right, red line). The grey-shaded area in **(c)** indicates the 1-σ uncertainty range of OS concentrations (on average ~40% during haze periods).

25

Figure 3. Production and existence of HMS in Beijing winter haze aerosols. (a) Schematic of heterogeneous HMS chemistry in northern China winter haze. **(b)** N_{HMS} (left, red line) and OS concentrations (right, black line). N_{HMS} was only available for a haze episode in December 2014 due to instrumentation constraints. **(c)** Gas-phase concentrations of observed SO_2 (left, black line) and modeled HCHO (right, blue line). **(d)** P_{HMS} (left, pink-shaded area) and P_{OS} (right, black line). The pink-shaded area shows the uncertainty of P_{HMS} due to the estimated range of pH (4.1–5.5). The inserted figure indicates the linear correlation of P_{HMS} and P_{OS} at a pH of 5.5.

26
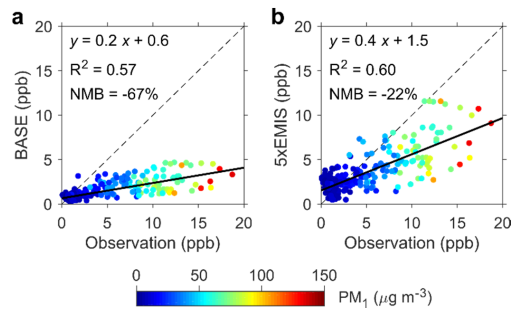
Figure 4. Comparison of modeled and observed HCHO concentrations. (a) BASE scenario. (b) 5×EMIS scenario. The dots are colored according to PM$_1$ concentrations. Model results from WRF-Chem are shown.

Supplement for acp-2018-1015

Shaojie Song et al. ~~2018~~2019

Supplementary Texts 1–4

Supplementary Figures 1–~~11~~12

5   Supplementary Tables 1–3

Supplementary Texts

Text S1. Uncertainty quantification of HR-AMS measurements

The HR-AMS measurement uncertainties were estimated following Bahreini et al.[1]. The relative uncertainty $\left(\frac{\Delta_X}{X}\right)$ of mass concentration of the chemical species X (i.e., ammonium, sulfate, nitrate, chloride, organics, and black carbon) was quantified as

$$\frac{\Delta_X}{X} = \sqrt{\left(\frac{\Delta_{\mathrm{IE_{NO_3}}}}{\mathrm{IE_{NO_3}}}\right)^2 + \left(\frac{\Delta_{\mathrm{RIE}_X}}{\mathrm{RIE}_X}\right)^2 + \left(\frac{\Delta_{\mathrm{CE}}}{\mathrm{CE}}\right)^2 + \left(\frac{\Delta_{\mathrm{Q}}}{\mathrm{Q}}\right)^2 + \left(\frac{\Delta_{\mathrm{TE}}}{\mathrm{TE}}\right)^2} \tag{S1}$$

where $\frac{\Delta_{\mathrm{IE_{NO_3}}}}{\mathrm{IE_{NO_3}}}, \frac{\Delta_{\mathrm{CE}}}{\mathrm{CE}}, \frac{\Delta_{\mathrm{Q}}}{\mathrm{Q}}$, and $\frac{\Delta_{\mathrm{TE}}}{\mathrm{TE}}$ represent the relative uncertainties in the nitrate ionization efficiency ($\mathrm{IE_{NO_3}}$), collection efficiency (CE), flow rate (Q), and transmission efficiency (TE), and were estimated to be 10%, 30%, <0.5%, and 10%, respectively. $\frac{\Delta_{\mathrm{RIE}_X}}{\mathrm{RIE}_X}$ represents the uncertainty in the ionization efficiency of the species X relative to nitrate (RIE_X), and depends on the species X (10% for ammonium, 15% for sulfate, and 20% for organics)[1]. Using the above equation, we estimated that the overall relative uncertainties of HR-AMS measurements were 33% (nitrate), 35% (ammonium), 36% (sulfate), and 39% (organics). The uncertainties for chloride were assumed to be 40%.

In order to quantify the uncertainty of sulfate-equivalent organosulfur concentration (C_{OS}), we rewrote Eq. (1) in the main text as

$$C_{\mathrm{OS}} = \frac{M_{\mathrm{SO_4^{2-}}}}{M_{\mathrm{SO^+}}}\left(1 + \frac{M_{\mathrm{SO^+}}}{M_{\mathrm{SO_2^+}}}\frac{\mathrm{SO_{2,OS}^+}}{\mathrm{SO_{OS}^+}}\right) \times \mathrm{SO_{OS}^+} \tag{S2}$$

$$\mathrm{SO_{OS}^+} = \left(1 - \left(\frac{R_{\mathrm{cd,SO^+/SO_3^+}}}{R_{\mathrm{obs,SO^+/SO_3^+}}} + \frac{R_{\mathrm{cd,SO^+/HSO_3^+}}}{R_{\mathrm{obs,SO^+/HSO_3^+}}} + \frac{R_{\mathrm{cd,SO^+/H_2SO_4^+}}}{R_{\mathrm{obs,SO^+/H_2SO_4^+}}}\right)/3\right) \times \mathrm{SO_{obs}^+} \tag{S3}$$

$$\mathrm{SO_{2,OS}^+} = \left(1 - \left(\frac{R_{\mathrm{cd,SO_2^+/SO_3^+}}}{R_{\mathrm{obs,SO_2^+/SO_3^+}}} + \frac{R_{\mathrm{cd,SO_2^+/HSO_3^+}}}{R_{\mathrm{obs,SO_2^+/HSO_3^+}}} + \frac{R_{\mathrm{cd,SO_2^+/H_2SO_4^+}}}{R_{\mathrm{obs,SO_2^+/H_2SO_4^+}}}\right)/3\right) \times \mathrm{SO_{2,obs}^+} \tag{S4}$$

where $\mathrm{SO_{OS}^+}$ and $\mathrm{SO_{2,OS}^+}$ are the concentrations of the $\mathrm{SO^+}$ and $\mathrm{SO_2^+}$ ions attributable to OS, respectively. The observed ion ratios are defined as $R_{\mathrm{obs,SO^+/SO_3^+}} = \frac{\mathrm{SO_{obs}^+}}{\mathrm{SO_{3,obs}^+}}$, $R_{\mathrm{obs,SO^+/HSO_3^+}} = \frac{\mathrm{SO_{obs}^+}}{\mathrm{HSO_{3,obs}^+}}$, $R_{\mathrm{obs,SO^+/H_2SO_4^+}} = \frac{\mathrm{SO_{obs}^+}}{\mathrm{H_2SO_{4,obs}^+}}$, $R_{\mathrm{obs,SO_2^+/SO_3^+}} = \frac{\mathrm{SO_{2,obs}^+}}{\mathrm{SO_{3,obs}^+}}$, $R_{\mathrm{obs,SO_2^+/HSO_3^+}} = \frac{\mathrm{SO_{2,obs}^+}}{\mathrm{HSO_{3,obs}^+}}$, and $R_{\mathrm{obs,SO_2^+/H_2SO_4^+}} = \frac{\mathrm{SO_{2,obs}^+}}{\mathrm{H_2SO_{4,obs}^+}}$. $R_{\mathrm{cd,SO^+/SO_3^+}}$, $R_{\mathrm{cd,SO^+/HSO_3^+}}$, $R_{\mathrm{cd,SO^+/H_2SO_4^+}}$, $R_{\mathrm{cd,SO_2^+/SO_3^+}}$, $R_{\mathrm{cd,SO_2^+/HSO_3^+}}$, and $R_{\mathrm{cd,SO_2^+/H_2SO_4^+}}$ represent the average ratios of the two corresponding ions in the clean and dry periods. We further defined A and B and rewrote Eq. (S2)

$$A = 1 - \left(\frac{R_{\mathrm{cd,SO^+/SO_3^+}}}{R_{\mathrm{obs,SO^+/SO_3^+}}} + \frac{R_{\mathrm{cd,SO^+/HSO_3^+}}}{R_{\mathrm{obs,SO^+/HSO_3^+}}} + \frac{R_{\mathrm{cd,SO^+/H_2SO_4^+}}}{R_{\mathrm{obs,SO^+/H_2SO_4^+}}}\right)/3 \tag{S5}$$

$$B = 1 - \left(\frac{R_{cd,SO_2^+/SO_3^+}}{R_{obs,SO_2^+/SO_3^+}} + \frac{R_{cd,SO_2^+/HSO_3^+}}{R_{obs,SO_2^+/HSO_3^+}} + \frac{R_{cd,SO_2^+/H_2SO_4^+}}{R_{obs,SO_2^+/H_2SO_4^+}}\right)/3 \tag{S6}$$

$$C_{OS} = \frac{M_{SO_4^{2-}}}{M_{SO^+}}\left(1 + \frac{M_{SO^+}}{M_{SO_2^+}}\frac{B}{A}R_{obs,SO_2^+/SO^+}\right) \times SO_{obs}^+ A \tag{S7}$$

where $R_{obs,SO_2^+/SO^+} = \frac{SO_{2,obs}^+}{SO_{obs}^+}$. The uncertainty of C_{OS} was calculated by propagating the uncertainties of each term in

Eqs. (S5–S7). The uncertainties of $R_{cd,SO^+/SO_3^+}$, $R_{cd,SO^+/HSO_3^+}$, $R_{cd,SO^+/H_2SO_4^+}$, $R_{cd,SO_2^+/SO_3^+}$, $R_{cd,SO_2^+/HSO_3^+}$, and $R_{cd,SO_2^+/H_2SO_4^+}$

5   were estimated by the standard deviations of the corresponding ion ratios observed during the clean and dry periods.

The uncertainties of $R_{obs,SO_2^+/SO^+}$, $R_{obs,SO^+/SO_3^+}$, $R_{obs,SO^+/HSO_3^+}$, $R_{obs,SO^+/H_2SO_4^+}$, $R_{obs,SO_2^+/SO_3^+}$, $R_{obs,SO_2^+/HSO_3^+}$, and

$R_{obs,SO_2^+/H_2SO_4^+}$ were obtained by the standard deviations of the 5-minute samples in each hour. The relative uncertainty

of SO_{obs}^+ was estimated by Eq. (S1) assuming the same RIE as sulfate.

10   **Text S2. Mass transfer of heterogeneous HMS production**

In order to examine whether the production of HMS was limited by the kinetics of mass transport, we estimated the

characteristic time scales (τ) for the HMS chemical reaction, the mass transfer steps (including gas-phase diffusion,

interfacial transport, hydrolysis/ionization, and aqueous-phase diffusion), and formaldehyde hydration. The average

values during winter haze episodes (PM$_1$ > 100 µg m^{-3}) were used in our calculation: $[SO_{2(g)}]$ = 14 ppb, $[HCHO_{(g)}]$

15   = 10 ppb, T = 278 K, PM$_1$ = 160 µg m^{-3}, and AWC = 100 µg m^{-3}. The characteristic times for the chemical loss of

SO$_2$ and HCHO, τ_{r,SO_2} and $\tau_{r,HCHO}$, were estimated by

$$\tau_{r,SO_2} = \{(k_1\alpha_1 + k_2\alpha_2)[HCHO_{(aq)}]\}^{-1} \text{ and } \tau_{r,HCHO} = \{(k_1\alpha_1 + k_2\alpha_2)[SO_{2(aq)}]\}^{-1} \tag{S8}$$

For a chemical species A (SO$_2$ or HCHO), the characteristic time, $\tau_{dg\&phase}$, that includes the gas-phase diffusion and

the establishment of phase equilibrium at the interface of aqueous aerosol particles was expressed as[2]

20   $$\tau_{dg\&phase} = \frac{H_A^* RT\rho_p R_p^2 \cdot AWC}{3m_p D_{g,A} f(Kn,\alpha)} \tag{S9}$$

where H_A^* is the effective Henry's law constant of A (M atm^{-1}), R is the gas constant, T is the temperature (K), ρ_p is

the aerosol droplet density and estimated to be 1.3×10^3 kg m^{-3}, R_p is the average aerosol droplet radius assumed as

0.15 µm following ref.[3], m_p is the aerosol droplet mass concentration (~260 µg m^{-3}), $D_{g,A}$ is the gas-phase diffusion

coefficient of A in the air (m^2 s^{-1})[4,5], and $f(Kn,\alpha)$ is the correction factor to mass transfer flux owing to non-continuum

25   effects and imperfect accommodation[6]

$$f(Kn,\alpha) = 0.75\alpha(1 + Kn)\left(Kn^2 + Kn + 0.283Kn\alpha + 0.75\alpha\right)^{-1} \tag{S10}$$

where α is the mass accommodation coefficient of A on aqueous surfaces, and the Knudsen number is given by

$$Kn = \frac{3D_{g,A}}{R_p}\sqrt{\frac{\pi M_A}{8RT}} \tag{S11}$$

3

where M_A is the molar mass of A. The characteristic time for aqueous-phase diffusion, τ_{da}, was quantified by[2]

$$\tau_{da} = \frac{R_p^2}{\pi^2 D_{aq}} \tag{S12}$$

where D_{aq} is the aqueous-phase diffusion coefficient (a typical value: 10^{-9} m^2 s^{-1}). The characteristic times, τ_{i1} and τ_{i2}, are respectively associated with the hydrolysis/ionization equilibria of $SO_{2(aq)}$ ($SO_2 \cdot H_2O \leftrightarrow HSO_3^- + H^+$ and $HSO_3^- \leftrightarrow SO_3^{2-} + H^+$) and were estimated following Schwartz and Freiberg[7]

$$\tau_{i1} = \{3 \times 10^6 \text{ s}^{-1} + 2 \times 10^8 \text{ M}^{-1} \text{ s}^{-1} \times ([H^+] + [HSO_3^-])\}^{-1} \tag{S13}$$

$$\tau_{i2} = \{2 \times 10^3 \text{ s}^{-1} + 3 \times 10^{10} \text{ M}^{-1} \text{ s}^{-1} \times ([H^+] + [SO_3^{2-}])\}^{-1} \tag{S14}$$

The characteristic time for the hydration of HCHO, τ_{hyd}, was estimated using the hydration rate constant k_{hyd} (s^{-1})

$$\tau_{hyd} = k_{hyd}^{-1} \tag{S15}$$

As shown in Fig. S1~~0~~1, the time scales of the mass transfer processes ($\tau_{dg\&phase}$, τ_{da}, τ_{i1}, and τ_{i2}) were much smaller than those of chemical reaction (τ_r) and HCHO hydration (τ_{hyd}), suggesting that the mass transfer and HCHO hydration were not rate-limiting for HMS production in aerosol water.

Text S3. Production of other hydroxyalkylsulfonate species

It is known that many aldehydes can undergo nucleophilic addition reactions with SO_2 to form HAS in the aqueous phase through a similar chemical mechanism with HCHO[8]. The importance of different aldehydes in the production of HAS depends on several factors including their gas-phase levels, water solubility, and kinetic and thermodynamic data. Most aldehydes already identified in the polluted atmosphere, such as acetaldehyde, propanal, butanal, pentanal, hexanal, and benzaldehyde, contribute insignificantly to HAS owing to low reaction rates. Four aldehydes, including glyoxal, methylglyoxal, glycolaldehyde, and glyoxylic acid, have similar or larger reaction rate constants compared to formaldehyde[8], and are thus worthy of further discussion. The properties of these aldehydes and their corresponding HAS species are given in Table S3.

In order to evaluate the relative importance of these aldehydes, we calculated their HAS formation rates, equilibrium concentrations, and characteristic times to reach equilibrium, using the average observational and model data ($[SO_{2(g)}]$ = 14 ppb, $[HCHO_{(g)}]$ = 10 ppb, T = 278 K, and AWC = 100 μg m^{-3}) obtained during Beijing winter haze periods (PM_1 > 100 μg m^{-3}). In the calculations, we assumed that these aldehydes had the same gaseous concentrations: $[RCHO_{(g)}]$ = 10 ppb. Although these aldehydes (methylglyoxal, glyoxal, glycolaldehyde, and glyoxylic acid) exhibited faster formation rates compared with formaldehyde, their equilibrium concentrations were much smaller, and it usually took less than a few hours for them to reach equilibrium (Fig. ~~S11~~S12). Also considering that their gas-phase concentrations are typically one to two orders of magnitude lower than that of formaldehyde in the polluted environment[9-11], we suggest that these aldehydes are much less important in the formation of HAS species compared to formaldehyde. In addition, the characteristic times to reach equilibrium for formaldehyde were found about 2–40

days for pH range of winter haze aerosols (4.1–5.5), larger than typical time scales of haze accumulation (less than a day)[12], and therefore, the HMS in aerosols were usually not in equilibrium with HCHO and SO_2 in the gas phase.

Text S4. Influence of ionic strength on HMS production

The relationship between the reaction rate constants (k) of HMS formation and the solution ionic strengths (I) has not been studied experimentally, and can only be estimated theoretically. The rate-limiting step of HMS production is the nucleophilic addition of an anion (HSO_3^- or SO_3^{2-}) to a neutral molecule (HCHO). For this type of reaction, the k–I relationship can be expressed by the kinetic salting coefficient b[13]

$$\log\left(k/k^{I=0}\right) = bI \tag{S16}$$

where $k^{I=0}$ represents the reaction rate constant in an ideal-dilute solution ($I = 0$ M). It is known that b is related to the water solubility of the neutral species[13] (i.e., HCHO), and according to ref.[14], the value of b is expected to be positive. Thus, the actual reaction rate constants (k) in aerosol water droplets (with an average I of ~11 M during haze periods) should be enhanced compared with dilute electrolyte solutions. It is noted that the kinetic salt effects may also depend on the nature of electrolytes present in the solution.

Supplementary Figures
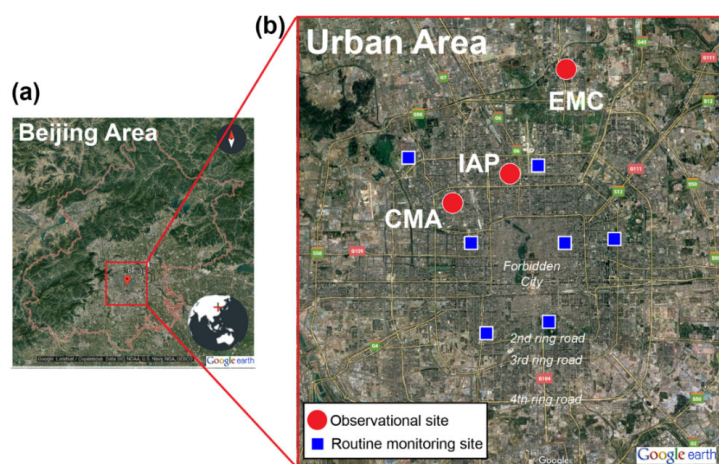
Figure S1. Location of observational sites in urban Beijing. (a) Map of Beijing area. (b) Sites in the urban area of Beijing city. The CMA, IAP, and EMC sites were located in the Chinese Academy of Meteorological Sciences (39.95°N, 116.33°E), the Institute of Atmospheric Physics of the Chinese Academy of Sciences (39.98°N, 116.38°E), and the China National Environmental Monitoring Centre (40.04°N, 116.42°E), respectively. The levels of air pollutants at the IAP site compared well with results from the routine urban monitoring sites of Beijing municipal environmental monitoring center (*www.bjmemc.com.cn*, last access: 24 September 2018), suggesting the homogeneity of air pollution in urban Beijing and the representativeness of observational sites.
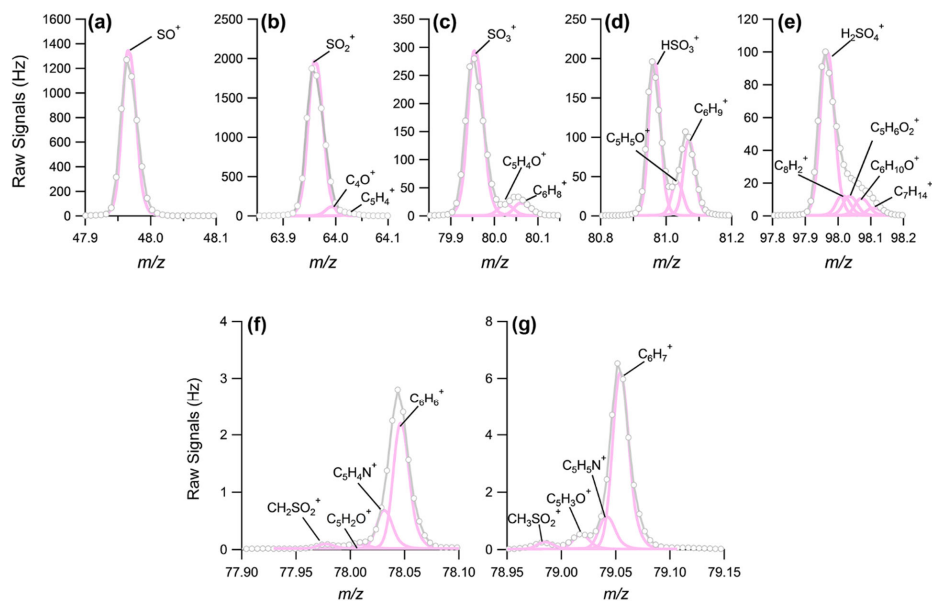
Figure S2. Examples of the raw signals and fitted peaks of inorganic and organic sulfur-containing fragment ions in the HR-AMS field measurements. (a) SO^+ (m/z 48), (b) SO_2^+ (m/z 64), (c) SO_3^+ (m/z 80), (d) HSO_3^+ (m/z 81), (e) $H_2SO_4^+$ (m/z 98), (f) $CH_2SO_2^+$ (m/z 78), and (g) $CH_3SO_2^+$ (m/z 79). (a–e) show the V-mode mass spectra data and (f–g) show the W-mode data.
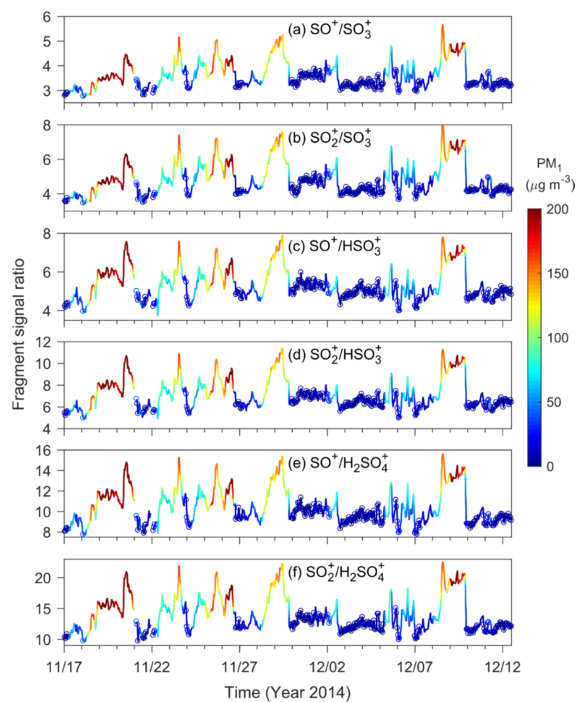
Figure S3. Time series of HR-AMS signal ratios of inorganic sulfur-containing fragment ions during winter 2014 in urban Beijing. (a) SO^+/SO_3^+, (b) SO_2^+/SO_3^+, (c) SO^+/HSO_3^+, (d) SO_2^+/HSO_3^+, (e) $SO^+/H_2SO_4^+$, and (f) $SO_2^+/H_2SO_4^+$. The circles indicate the observations under clean and dry conditions (filtered by $PM_1 < 50$ µg m^{-3}, RH < 30%, and $O_3 > 10$ ppb). The curves and circles are colored according to the observed PM_1 concentrations. The haze conditions are defined as $PM_1 > 100$ µg m^{-3}.

Formatted: Justified, Space After: 10 pt, Line spacing: single
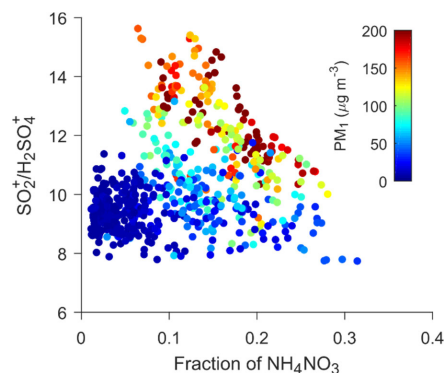
Figure S4. Relationship between $SO_2^+/H_2SO_4^+$ and fraction of ammonium nitrate. The dots are colored according to PM_1 mass concentrations.

5
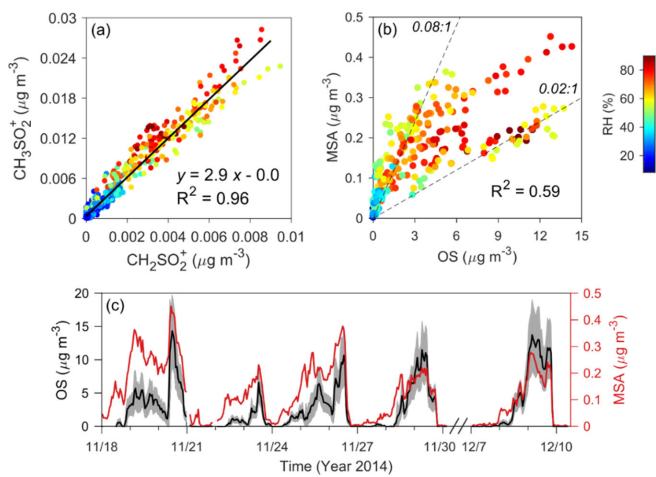
Figure S4S5. Methanesulfonate (or MSA) in Beijing winter aerosols estimated by HR-AMS. (a) Linear correlation of the observed hourly concentrations of fragment ions $CH_3SO_2^+$ and $CH_2SO_2^+$. (b) Scatter plot and (c) Time series of the identified sulfate-equivalent OS and methanesulfonate (or MSA) concentrations. The dots in (a–b) are colored according to RH. The shaded region in (c) indicates the 1-σ uncertainty range of OS.

10

9
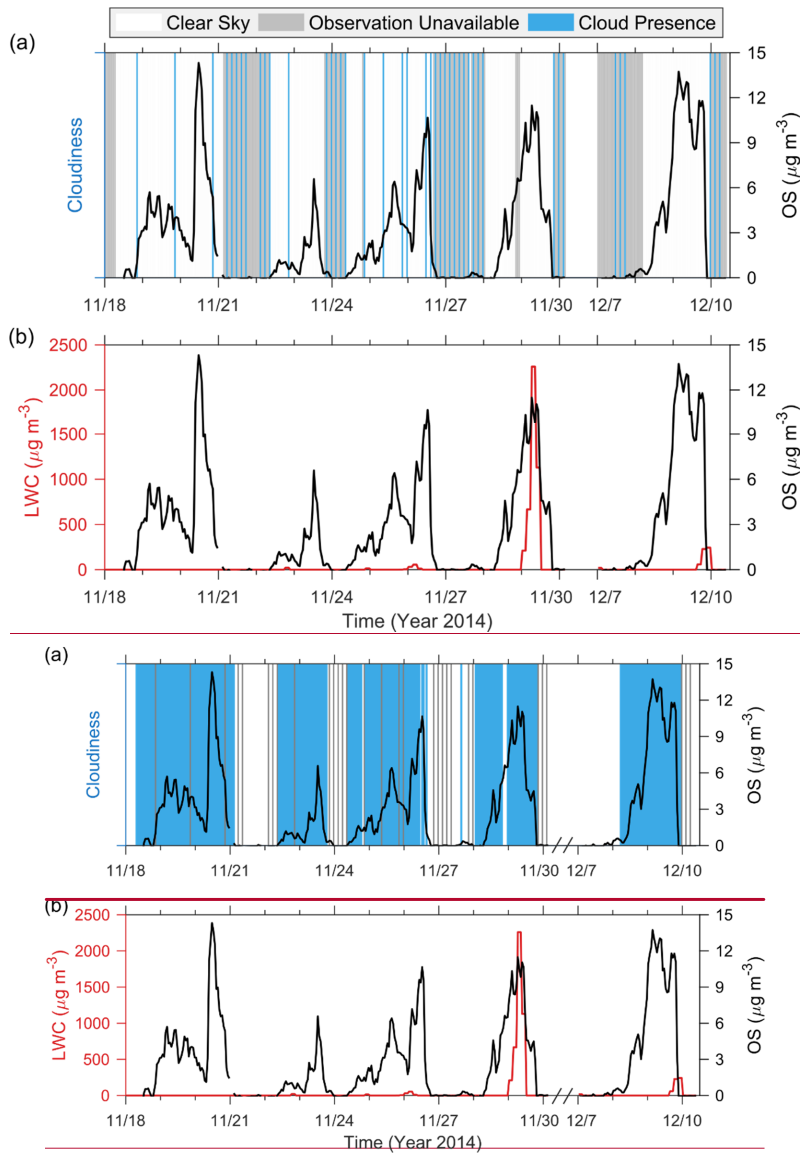
Figure S5S6. Relationship between the sulfate-equivalent OS concentrations and cloud/fog information in Beijing winter. (a) Time series of OS and cloud cover as observed at the Beijing Capital International Airport. Blue, ~~grey~~white,

and ~~white~~ gray colors indicate cloud presence, clear sky, ~~cloud presence,~~ and observation unavailable, respectively. Cloud cover data were obtained from the NOAA's National Climatic Data Center (NCDC) Integrated Surface Database (ISD)[15]. (b) Time series of OS and cloud/fog liquid water content (LWC) during 2014 winter in Beijing. LWC was obtained from the MERRA-2 reanalysis meteorology (Modern-Era Retrospective analysis for Research and Applications, Version 2)[16]. The average LWC over the Beijing area and below 1 km (assumed as the upper limit of the planetary boundary layer height during Beijing winter haze periods[17-19]) is calculated and shown.
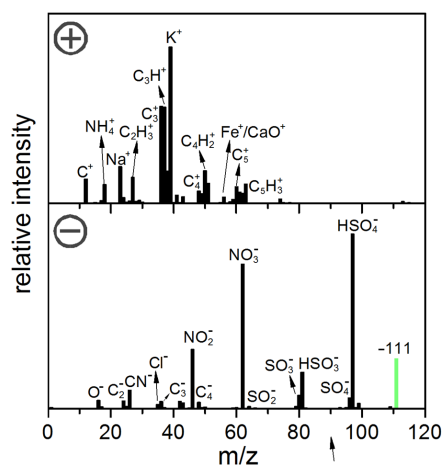
Figure S6S7. Average positive (+) and negative (−) ion mass spectra of HMS-containing individual particles from the SPAMS analysis. The m/z −111 peak was attributed to HMS. The m/z −81 HSO_3^-, m/z −80 SO_3^-, and m/z −64 SO_2^- peaks likely resulted from the fragmentation of HMS. The negative mass spectra also suggested the presence of nitrate (m/z −46 NO_2^- and m/z −62 NO_3^-), sulfate (m/z −96 SO_4^- and m/z −97 HSO_4^-), and carbonaceous species (e.g., m/z −16 O^-, m/z −24 C_2^-, and m/z −26 CN^-). The positive mass spectra featured m/z +18 NH_4^+, m/z +39 K^+, m/z +23 Na^+, and carbonaceous species (e.g., m/z +21 C^+ and m/z +27 $C_2H_3^+$). The response of different species varied in the single particle mass spectrometry owing to their difference in ionization energy and matrix effects. Some species such as Na^+ and K^+ were more sensitive in the mass spectra because their ionization energies are low[20].
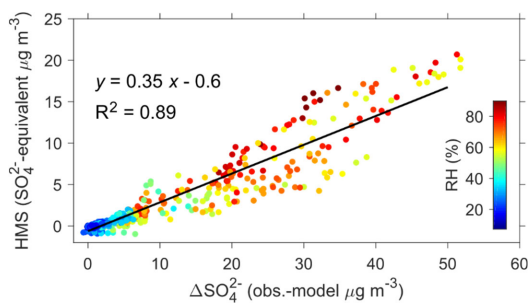

Figure S7S8. Contribution of HMS to the missing sulfate (ΔSO_4^{2-}) concentrations, if the identified OS resided only in the form of HMS. The HR-AMS mass spectra of standard HMS obtained from refs.[21,22] were used for estimation.
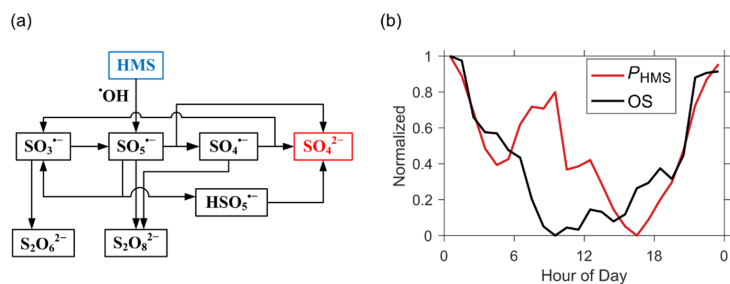
Figure S8S9. The possible role of HMS chemistry in the missing sulfate problem. (a) Schematic of reactions in the radical oxidation chain of HMS by the OH radical. (b) Average normalized diurnal profiles of HMS production rate (P_{HMS}) and OS concentrations.

5
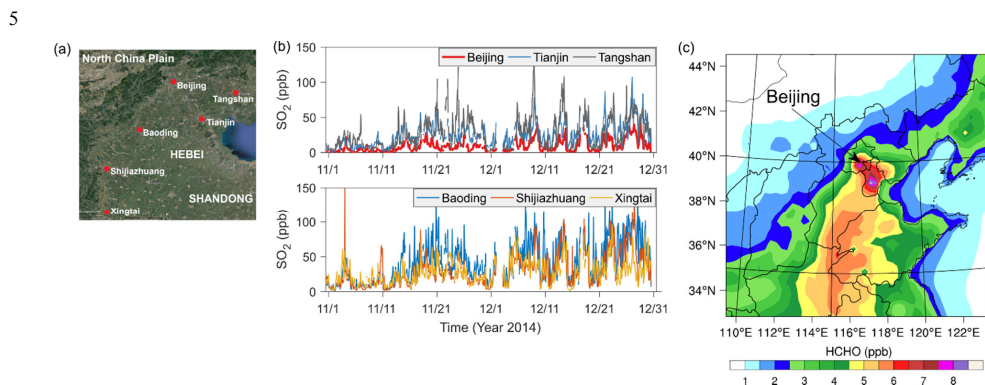
Figure S9S10. Regional pollution of SO_2 and HCHO across the NCP during winter 2014. (a) Topographic map around Beijing, and location of cities shown in (b). (b) SO_2 concentrations in Beijing and its southwest and southeast cities. (c) Distribution of HCHO from WRF-Chem model simulations.
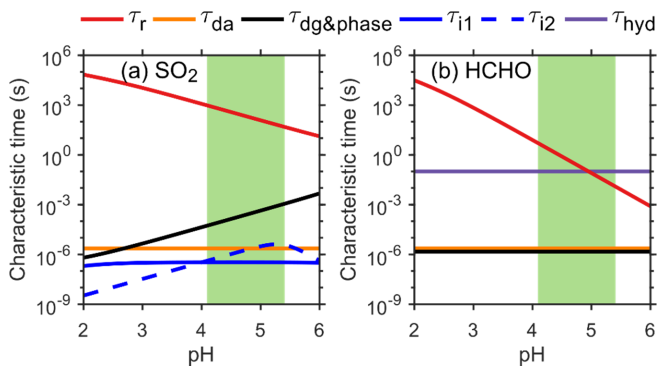
Figure S10S11. The characteristic times of mass transfer and chemical reaction for HMS production. (a) and (b) show the characteristic time scales (τ) of SO_2 and HCHO, respectively (defined in Text S2). The green shaded regions indicate the relevant aerosol water pH range of winter haze.
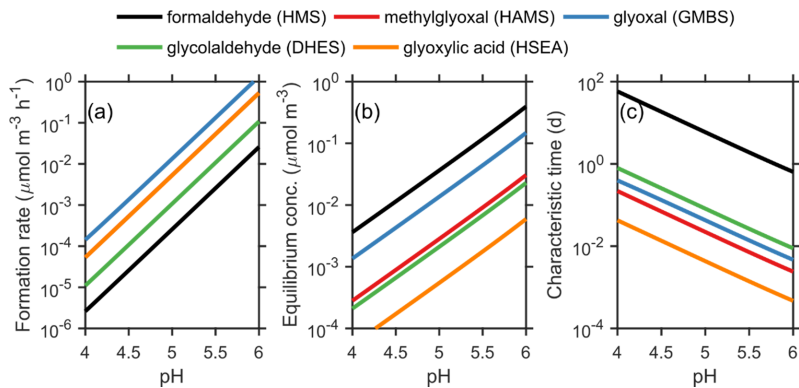
Figure S11S12. Comparison of the relative importance of several aldehydes in the formation of HAS. (a), (b), and (c) respectively show the calculated HAS formation rates, equilibrium concentrations, and characteristic times to reach equilibrium for five aldehydes (formaldehyde, methylglyoxal, glyoxal, glycolaldehyde, and glyoxylic acid), using the average measurement and model data obtained during Beijing winter haze periods (2014 winter).

Supplementary Tables

Table S1. Summary of experimental methods in the field measurements.

Species	Instrument	Site	Time resolution	Period (2014)
PM_1, ammonium, sulfate, nitrate, chloride, organics, and S-containing fragment ions	High-resolution time-of-flight aerosol mass spectrometer (HR-AMS; Aerodyne Research, Inc., USA)	IAP	5 min	11/17 to 12/12
$PM_{0.2-2}$, fragment ions at different m/z	Single particle aerosol mass spectrometer (SPAMS; Hexin Analytical Instrument Co., China)	EMC	10 min	12/4 to 12/12
$PM_{2.5}$, black carbon	Aethalometer Model AE33	IAP	1 min	11/17 to 12/12
Gas NH_3, HNO_3, and HCl	Gas and Aerosol Collector Ion Chromatography (GAC-IC)	IAP	30 min	11/17 to 12/12
Gas HCHO	AL4021 analyzer (Aero Laser GmbH, Germany)	CMA	2 min	12/1 to 12/15
Gas SO_2 and O_3	Model 43i and 49i analyzers (Thermo Fisher Scientific Inc., USA)	IAP	1 min	11/17 to 12/15
Temperature and relative humidity	Rotronic HC2-S3 probe	IAP	1 min	11/17 to 12/15

Table S2. Physical and chemical constants of SO_2.

Symbol	Value	Note	Source
α, dimensionless	0.11	Mass accommodation coefficient on aqueous surfaces	ref. [2]
H_{298}, M atm^{-1} ($-\Delta H/R$, K)	1.3 (3100)	$SO_{2(g)} + H_2O \leftrightarrow SO_2 \cdot H_2O$	ref. [23]
K_{s1}, M ($-\Delta H/R$, K)	1.3×10^{-2} (2000)	$SO_2 \cdot H_2O \overset{K_{s1}}{\leftrightarrow} HSO_3^- + H^+$	ref. [2]
K_{s2}, M ($-\Delta H/R$, K)	6.6×10^{-8} (1500)	$HSO_3^- \overset{K_{s2}}{\leftrightarrow} SO_3^{2-} + H^+$	ref. [2]

The dependence of H at a given temperature T is expressed below and similar expressions apply to K_{s1} and K_{s2}.

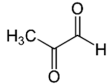$$H(T) = H_{298} \exp\left[\frac{-\Delta H}{R}\left(\frac{1}{T} - \frac{1}{298}\right)\right]$$

The fractions of HSO_3^- and SO_3^{2-} in $SO_{2(aq)}$, α_1 and α_2, respectively, are determined by

$$\alpha_1 = \frac{K_{s1}[H^+]}{[H^+]^2 + K_{s1}[H^+] + K_{s1}K_{s2}} \text{ and } \alpha_2 = \frac{K_{s1}K_{s2}}{[H^+]^2 + K_{s1}[H^+] + K_{s1}K_{s2}}$$

where K_{s1} and K_{s2} are the corresponding acid dissociation constants (M), and $[H^+]$ refers to the hydrogen ion activity (M).

5

Table S3. Physical and chemical properties of several aldehydes and their corresponding hydroxyalkylsulfonates.

	Aldehydes (RCHO)				
Aldehyde	formaldehyde	methylglyoxal	glyoxal[a]	glycolaldehyde	glyoxylic acid[b]
Other name(s)	methanal	pyruvaldehyde; propanonal	ethanedial	hydroxyacetaldehyde; 2-hydroxyethanal	oxoacetic acid; oxoethanoic acid
Formula	HCHO	CH₃COCHO	CHOCHO	HOCH₂CHO	HO₂CCHO
Structure					
H_{298}, **M atm^{-1} ($-\Delta H/R$, K)**	2.5^c (3300^d)	1.4^c (N.A.)	1.9^e (N.A.)	4.1×10^{3c} (N.A.)	29^e (N.A.)
H^*_{298}, **M atm^{-1} ($-\Delta H/R$, K)**	3.2×10^{3f} (7100^f)	3.7×10^{3c} (7500^c)	4.1×10^{5f} (7500^f)	4.1×10^{4c} (4600^c)	1.1×10^{4f} (4800^f)
k_{hyd} **at 298 K, s^{-1}**	$10^{g,h}$	20^g	10^i	N.A.	10^g
α, **dimensionless**	0.02^j	$\geqslant 1 \times 10^{-4k}$	0.02^i	N.A.	N.A.

	Hydroxyalkylsulfonates (HAS)				
Hydroxyalkylsulfonate	hydroxymethanesulfonate	hydroxyacetylmethanesulfonate	1-hydroxy-2,2-diol-1-ethanesulfonate (or glyoxal monobisulfite)	1,2-dihydroxy-1-ethanesulfonate	2-hydroxy-2-sulfo-ethanoic acid
Abbreviation	HMS	HAMS	GMBS[a]	DHES	HSEA
Formula	CH₂(OH)SO₃⁻	CH₃COCH(OH)SO₃⁻	CH(OH)₂CH(OH)SO₃⁻	CH₂(OH)CH(OH)SO₃⁻	HO₂CCH(OH)SO₃⁻
k_1, **M^{-1} s^{-1} ($-E/R$, K)**	7.9×10^2 (-4900)^l	3.5×10^3 (-3500)^m	3×10^4 (N.A.)^n	1.7 (-3600)^o	4.4×10^2 (-2600)^p
k_2, **M^{-1} s^{-1} ($-E/R$, K)**	2.5×10^7 (-1800)^l	3.7×10^8 (-2200)^m	4×10^8 (N.A.)^n	5.0×10^4 (-2100)^o	2.0×10^7 (N.A.)^p
K_{eq}, **M^{-1} ($-\Delta H/R$, K)**	$(5-9) \times 10^9$ (10000)^q	8×10^8 (6600)^m	6×10^9 (3500)^n	2×10^6 (N.A.)^g	7×10^7 (N.A.)^p

N.A. = not available. H, H^*, and K_{eq} have similar expressions of temperature dependence as those for SO_2. The temperature dependence of the reaction rate constants k (k_1 or k_2) is

$$k(T) = k(298) \exp\left(\frac{-E}{R}\left(\frac{1}{T} - \frac{1}{298}\right)\right)$$

[a]The mechanism for glyoxal is more complicated than those for other aldehydes as glyoxal has two aldehyde groups. Both free CHOCHO and its monohydrated form CH(OH)$_2$CHO can react with SO$_{2(aq)}$ to form hydroxyalkylsulfonates: CHOCHO + HSO$_3^-$ ↔ CHOCH(OH)SO$_3^-$, CHOCHO + SO$_3^{2-}$ ↔ CHOCH(O$^-$)SO$_3^-$, CH(OH)$_2$CHO + HSO$_3^-$ ↔ CH(OH)$_2$CH(OH)SO$_3^-$, and CH(OH)$_2$CHO + SO$_3^{2-}$ ↔ CH(OH)$_2$CH(O$^-$)SO$_3^-$. The intrinsic rate constants for the above individual nucleophilic addition reactions were not determined, whereas the apparent rate constants for the total dissolved glyoxal (CHOCHO + CH(OH)$_2$CHO + (CH(OH)$_2$)$_2$) were obtained in laboratory experiments[24]. For the sake of simplicity, we assume that the nucleophilic addition of CH(OH)$_2$CHO is insignificant compared with CHOCHO, and, accordingly, the intrinsic rate constants for CHOCHO + HSO$_3^-$ ↔ CHOCH(OH)SO$_3^-$ and CHOCHO + SO$_3^{2-}$ ↔ CHOCH(O$^-$)SO$_3^-$ can be derived from the apparent rate constants and the equilibrium constants of glyoxal hydration[23-25]. It is important to note that this simplification may lead to an overestimation of the actual formation rates of GMBS, and therefore the listed values of k_1 and k_2 should be regarded as the upper limits. GMBS can further react with SO$_{2(aq)}$ to form GDBS (1,2-dihydroxy-1,2-ethanesulfonate or glyoxal dibisulfite, (CH(OH)SO$_3^-$)$_2$): GMBS + SO$_{2(aq)}$ ↔ GDBS. The formation of GDBS is not considered since the kinetic and thermodynamic data remain unclear.

[b]Glyoxylic acid may dissociate in aqueous solution, HO$_2$CCHO ↔ H$^+$ + $^-$O$_2$CCHO, with a pK_a of about 2[26]. Note that HO$_2$CCHO is the reactive carbonyl species and that $^-$O$_2$CCHO does not contribute significantly to the nucleophilic addition with SO$_{2(aq)}$.[8] HSEA may dissociate in aqueous solution, HO$_2$CCH(OH)SO$_3^-$ ↔ H$^+$ + $^-$O$_2$CCH(OH)SO$_3^-$, with a pK_a of about 3[26].

[c]From the compilation by ref. [27].

[d]Inferred from $-\Delta H/R = 7100$ K for the effective Henry's law constant H^* and $-\Delta H/R = 3800$ K for the hydration equilibrium constant HCHO + H$_2$O ↔ CH$_2$(OH)$_2$[23,28].

[e]Ref. [25].

[f]From the compilation by ref. [23].

[g]From the compilation by ref. [8].

[h]Ref. [28] derived an expression for the reaction rate constant of formaldehyde hydration: $k_{hyd} = 2.0 \times 10^5 \times \exp(-2900/T)$ s^{-1}, which decreases with the ambient temperature.

[i]Ref. [29]. k_{hyd} data are for the first step hydration of glyoxal: CHOCHO + H$_2$O ↔ CH(OH)$_2$CHO.

[j]From the compilation by ref. [2].

[k]From the compilation by ref. [30].

[l]Ref. [31]. Experiments were conducted at $I = 1.0$ M, $0.7 \leq$ pH ≤ 3.5.

[m]Ref. [32]. Experiments were conducted at $I = 0.2$ M, $0.7 \leq$ pH ≤ 2.

[n]Ref. [24]. Experiments were conducted at $I = 0.2$ M, $0.7 \leq$ pH ≤ 3.3.

[o]Ref. [33]. Experiments were conducted at $I = 0.2$ M, $0.7 \leq$ pH ≤ 3.3.

[p]Ref. [26]. Experiments were conducted at $I = 0.2$ M, $0.7 \leq$ pH ≤ 2.9.

[q]Derived from ref. [28,34-36]. K_{eq} remains unchanged over the pH range from 3 to 7 (when HSO$_3^-$ is the dominant SO$_{2(aq)}$ species).

Supplementary References

1.   Bahreini, R. et al. Organic aerosol formation in urban and industrial plumes near Houston and Dallas, Texas. *J. Geophys. Res.-Atmos.* **114**, D00F16 (2009).

2.   Seinfeld, J. H., Pandis, S. N. *Atmospheric chemistry and physics: from air pollution to climate change*, Third edn. John Wiley & Sons, Inc. (2016).

3.   Cheng, Y. et al. Reactive nitrogen chemistry in aerosol water as a source of sulfate during haze events in China. *Sci. Adv.* **2**, e1601530 (2016).

4.   Kimbell, J. S., Subramaniam, R. P., Gross, E. A., Schlosser, P. M., Morgan, K. T. Dosimetry modeling of inhaled formaldehyde: comparisons of local flux predictions in the rat, monkey, and human nasal passages. *Toxicol. Sci.* **64**, 100-110 (2001).

5.   Tang, M. J., Cox, R. A., Kalberer, M. Compilation and evaluation of gas phase diffusion coefficients of reactive trace gases in the atmosphere: volume 1. Inorganic compounds. *Atmos. Chem. Phys.* **14**, 9233-9247 (2014).

6.   Fuchs, N. A., Sutugin, A. G. High-dispersed aerosols. In: *Topics in Current Aerosol Research* (eds Brock J. R.). Pergamon (1971).

7.   Schwartz, S. E., Freiberg, J. E. Mass-transport limitation to the rate of reaction of gases in liquid droplets: Application to oxidation of SO_2 in aqueous solutions. *Atmos. Environ.* **15**, 1129-1144 (1981).

8.   Olson, T. M., Hoffmann, M. R. Hydroxyalkylsulfonate formation: Its role as a S(IV) reservoir in atmospheric water droplets. *Atmos. Environ.* **23**, 985-997 (1989).

9.   Lui, K. H. et al. Spatial distributions of airborne di-carbonyls in urban and rural areas in China. *Atmos. Res.* **186**, 1-8 (2017).

10. Rao, Z., Chen, Z., Liang, H., Huang, L., Huang, D. Carbonyl compounds over urban Beijing: concentrations on haze and non-haze days and effects on radical chemistry. *Atmos. Environ.* **124**, 207-216 (2016).

11. Huang, X. H. H., Ip, H. S. S., Yu, J. Z. Secondary organic aerosol formation from ethylene in the urban atmosphere of Hong Kong: A multiphase chemical modeling study. *J. Geophys. Res. Atmos.* **116**, D03206 (2011).

12. Sun, Y. et al. Rapid formation and evolution of an extreme haze episode in Northern China during winter 2015. *Sci. Rep.* **6**, 27151 (2016).

13. Herrmann, H. Kinetics of aqueous phase reactions relevant for atmospheric chemistry. *Chem. Rev.* **103**, 4691-4716 (2003).

14. Toda, K. et al. Formaldehyde content of atmospheric aerosol. *Environ. Sci. Technol.* **48**, 6636-6643 (2014).

15. Smith, A., Lott, N., Vose, R. The integrated surface database: recent developments and partnerships. *Bull. Amer. Meteor. Soc.* **92**, 704-708 (2011).

16. Global Modeling and Assimilation Office (GMAO). MERRA-2 tavg3_3d_cld_Np: 3d,3-Hourly,Time-Averaged,Pressure-Level,Assimilation,Cloud Diagnostics V5.12.4, Greenbelt, MD, USA, Goddard Earth Sciences Data and Information Services Center (GES DISC), Accessed [05/16/2018]. (2015).

17. Luan, T., Guo, X., Guo, L., Zhang, T. Quantifying the relationship between $PM_{2.5}$ concentration, visibility and planetary boundary layer height for long-lasting haze and fog–haze mixed events in Beijing. *Atmos. Chem. Phys.* **18**, 203-225 (2018).

18. Tie, X. et al. Severe pollution in China amplified by atmospheric moisture. *Sci. Rep.* **7**, 15760 (2017).

19. Zhong, J. et al. Feedback effects of boundary-layer meteorological factors on cumulative explosive growth of $PM_{2.5}$ during winter heavy pollution episodes in Beijing from 2013 to 2016. *Atmos. Chem. Phys.* **18**, 247-258 (2018).

20. Gross, D. S., Gälli, M. E., Silva, P. J., Prather, K. A. Relative sensitivity factors for alkali metal and ammonium cations in single-particle aerosol time-of-flight mass spectra. *Anal. Chem.* **72**, 416-422 (2000).

21. Ge, X., Zhang, Q., Sun, Y., Ruehl, C. R., Setyan, A. Effect of aqueous-phase processing on aerosol chemistry and size distributions in Fresno, California, during wintertime. *Environ. Chem.* **9**, 221-235 (2012).

22. Gilardoni, S. et al. Direct observation of aqueous secondary organic aerosol from biomass-burning emissions. *Proc. Natl. Acad. Sci. U.S.A.* **113**, 10013-10018 (2016).

23. Sander, R. Compilation of Henry's law constants (version 4.0) for water as solvent. *Atmos. Chem. Phys.* **15**, 4399-4981 (2015).

24. Olson, T. M., Hoffmann, M. R. Kinetics, mechanism and thermodynamics of glyoxal-sulfur(IV) adduct formation. *J. Phys. Chem.* **92**, 533-540 (1988).

25. Ip, H. S. S., Huang, X. H. H., Yu, J. Z. Effective Henry's law constants of glyoxal, glyoxylic acid, and glycolic acid. *Geophys. Res. Lett.* **36**, L01802 (2009).

26. Olson, T. M., Hoffmann, M. R. Formation kinetics, mechanism, and thermodynamics of glyoxylic acid-sulfur(IV) adducts. *J. Phys. Chem.* **92**, 4246-4253 (1988).

27. Betterton, E. A., Hoffmann, M. R. Henry's law constants of some environmentally important aldehydes. *Environ. Sci. Technol.* **22**, 1415-1418 (1988).

28. Winkelman, J. G. M., Voorwinde, O. K., Ottens, M., Beenackers, A. A. C. M., Janssen, L. P. B. M. Kinetics and chemical equilibrium of the hydration of formaldehyde. *Chem. Eng. Sci.* **57**, 4067-4076 (2002).

29. Ervens, B., Volkamer, R. Glyoxal processing by aerosol multiphase chemistry: towards a kinetic modeling framework of secondary organic aerosol formation in aqueous particles. *Atmos. Chem. Phys.* **10**, 8219-8244 (2010).

30. Sander, S. P., J. Abbatt, J. R. Barker, J. B. Burkholder, R. R. Friedl, D. M. Golden, R. E. Huie, C. E. Kolb, M. J. Kurylo, G. K. Moortgat, V. L. Orkin, P. H. Wine,. Chemical kinetics and photochemical data for use in atmospheric studies, evaluation no. 17. JPL Publication 10-6, Jet Propulsion Laboratory, Pasadena, http://jpldataeval.jpl.nasa.gov (2011).

31. Boyce, S. D., Hoffmann, M. R. Kinetics and mechanism of the formation of hydroxymethanesulfonic acid at low pH. *J. Phys. Chem.* **88**, 4740-4746 (1984).

32. Betterton, E. A., Hoffmann, M. R. Kinetics, mechanism and thermodynamics of the reversible reaction of methylglyoxal (CH_3COCHO) with sulfur(IV). *J. Phys. Chem.* **91**, 3011-3020 (1987).

33. Olson, T. M., Torry, L. A., Hoffmann, M. R. Kinetics of the formation of hydroxyacetaldehyde-sulfur(IV) adducts at low pH. *Environ. Sci. Technol.* **22**, 1284-1289 (1988).

34.   Deister, U., Neeb, R., Helas, G., Warneck, P. Temperature dependence of the equilibrium $CH_2(OH)_2 + HSO_3^-$ $= CH_2(OH)SO_3^- + H_2O$ in aqueous solution. *J. Phys. Chem.* **90**, 3213-3217 (1986).

35.   Dong, S., Dasgupta, P. K. On the formaldehyde-bisulfite-hydroxymethanesulfonate equilibrium. *Atmos. Environ.* **20**, 1635-1637 (1986).

36.   Kok, G. L., Gitlin, S. N., Lazrus, A. L. Kinetics of the formation and decomposition of hydroxymethanesulfonate. *J. Geophys. Res. Atmos.* **91**, 2801-2804 (1986).